Responses to Reviewers' Comments

We sincerely appreciate the time and effort devoted by the reviewers and editor. We thank the reviewers for these constructive and professional comments. Our point-to-point responses can be found below. The reviewer comments/suggestions are in *italic* font, and our responses are underlined and in blue. The file name "Manuscript with marked changes" is abbreviated as "mms".

Referee #1 Evaluations (Eric Bruning):

The authors analyze a single case study of an isolated thunderstorm over land to the northeast of Guangzhou, China. Analysis of differential reflectivity and specific differential phase columns over the lifecycle of this storm allows the authors to analyze how the cloud microphysics lead to lightning, and the lead time that polarimetric radar allows in inferring the onset of lightning.

The case study largely repeats previous findings. There are a few valuable advancements in analysis methods (column identification methodology; inferring supercooled rain water content using a method from the late 1990s / early 2000s; lead time calculations by different methods). There are also some process inferences related to different pathways by which lightning might be produced that could be valuable and clarifying, but the universality of which is hard to judge on the basis of a single case study.

The authors have therefore engaged substantively in an ongoing tradition of analysis of polarimetric radar and lightning signals, with fair-to-good scientific significance, and good scientific and presentation quality. Below I note additional areas that could improve the manuscript, adding some missing information and clarifying the interpretation.

We sincerely appreciate your evaluation and insightful comments, which helped us improve this manuscript. The comparison between this study and your results is valuable for deepening our knowledge of the polarimetric structures related to lightning activity.

Major comments

1) *The authors do a nice job of reviewing the literature. I wanted to also mention our just-published paper, Bruning et al. (2024, 10.1175/MWR-D-24-0060.1), which pursues a very similar analysis on a large sample of storms. The authors' detailed look at the time-series perspective here is valuable (and something we did not yet*

do), and I would be interested to see where this study fits in the distribution of lightning and polarimetry of storms sampled by Bruning et al., which were probably similar small, isolated, subtropical storms.

Reply: We have added more discussion about this study fits in the distribution of lightning and polarimetry of storms sampled by Bruning et al. (2024), which were probably similar small, isolated, subtropical storms. Moreover, more cases have been added to strengthen our results (Table 1, including the original analysis case in the manuscript). In addition, the results revealed in this study are discussed with those of Sharma et al. (2024) and Sharma et al. (2021). Please see in mms (Lines 194−199; 579−639; 719−748).

Table 1. The information of cases

Cases number	Time information [CST]	CAPE [J kg^{-1}]
#1	17:18 to 19:00, 20 June 2016	1277
#2	12:12 to 13:18, 26 June 2016	1225
#3	15:36 to 16:36, 3 July 2016	961
#4	16:06 to 17:06, 5 July 2016	412
#5	11:00 to 12:12, 6 July 2016	1202
#6	16:18 to 17:06, 6 July 2016	1202
#7	15:00 to 16:06, 16 July 2016	1425
#8	13:24 to 14:12, 27 July 2016	1203
#9	14:36 to 15:18, 27 July 2016	1376
#10	14:54 to 15:18, 27 July 2016	1286
#11	13:24 to 15:00, 29 May 2016	1339
#12	09:18 to 10:48, 18 June 2016	1437
#13	12:18 to 13:00, 18 June 2016	1375
#14	15:48 to 16:36, 18 June 2016	1475
#15	13:06 to 14:12, 7 July 2016	2537

In our study, these 15 cases involved isolated thunderstorm cells, which produced lightning. Each of them has a Z_{DR} column; however, the absence of a K_{DP} column is possible (Figure 5a and b, Figure 10 a1-a7, b1-b7, Figure 11 a1-a7, b1-b7). The results of our study support the observations of Bruning et al. (2024), namely, that lightning is not observed in the absence of a Z_{DR} column and that a K_{DP} column is not observed without a Z_{DR} column. Moreover, the highest lightning flash frequency (in case #11) is observed when the Z_{DR} and K_{DP} columns are co-present, which is consistent with the observations of Bruning et al. (2024).

In addition, our results suggest that the signal in the K_{DP} column within these small, isolated, subtropical thunderstorms over South China is not as steady as that in the Z_{DR} column during the life cycle.

To further explore the characteristics of the microphysics related to the Z_{DR}/K_{DP} column and lightning within these thunderstorms, hydrometeor identification method involving

the fuzzy-logic algorithm (as in Zhao et al., 2021b) and the microphysical fingerprint (following Kumjian et al., 2022) are conducted. Identifying polarimetric radar "fingerprints" of ongoing microphysical processes was introduced by Kumjian (2012); these fingerprints are defined as vertical changes in two (e.g., Z_H, Z_{DR}) or more of the dual-polarization radar variables (Kumjian et al., 2022). More detail can be found in **Section 2.2** and **Section 3.2**.

Lines 194−199 in mms:

"This study included 15 isolated thunderstorm cells that produced lightning, which was observed via an S-band dual-polarization radar deployed in Guangzhou city (GZ radar) and a low-frequency E-field detection array (LFEDA) (Table 1). The average 6-hourly convective available potential energy (CAPE) of these thunderstorms was obtained from ERA-Interim reanalysis data, as in Zhao et al. (2022). The detailed examination of lightning activity with related dynamics and microphysics in case #1 was conducted first, and then the statistical results of all cases were given."

Lines 579−639 in mms:

"**3.4. Statistical results**

To determine the relationship between lightning activity and the quantified Z_{DR} columns, the height and volume of the Z_{DR} column are calculated via the "3D mapping column" method; the volume is based on the accumulation of all grids within the Z_{DR} column, and the volume of a single grid is 0.03125 km^3, with 0.25-km horizontal and 500-m vertical resolutions. The height of the Z_{DR} column is determined by counting the grid number (n) from the melting level to the highest grid within the Z_{DR} column; if n is determined, the Z_{DR} column height is n×0.5 km.

The variations in the Z_{DR}/K_{DP} column height and volume with the life cycle of the remaining fourteen cases are displayed in Figures 10 (cases #2 to #8) and 11 (cases #9 to #15), as are the variations in the percentages of hydrometeor types and microphysical fingerprints. The grid is assigned to specific particle type based on the results of hydrometeor identification, and the percentage of grids for each hydrometeor type is calculated. Similarly, this process is applied to determine the percentage of grids associated with microphysical fingerprints. Each of them has a Z_{DR} column (Figure 10 a1-a7, Figure 11 a1-a7); however, the absence of a K_{DP} column is possible (Figures 10 b1-b7, Figures 11 b1-b7). The results of our study support the observations of Bruning et al. (2024), namely, lightning is not observed in the absence of a Z_{DR} column, and a K_{DP} column is not observed without a Z_{DR} column. Moreover, the highest

lightning flash frequency (in case #11) is observed when the Z_{DR} and K_{DP} columns are co-present, which is consistent with the observations of Bruning et al. (2024). In addition, our results suggest that the signal in the K_{DP} column within these small, isolated, subtropical thunderstorms over South China is not as steady as that in the Z_{DR} column during the life cycle.

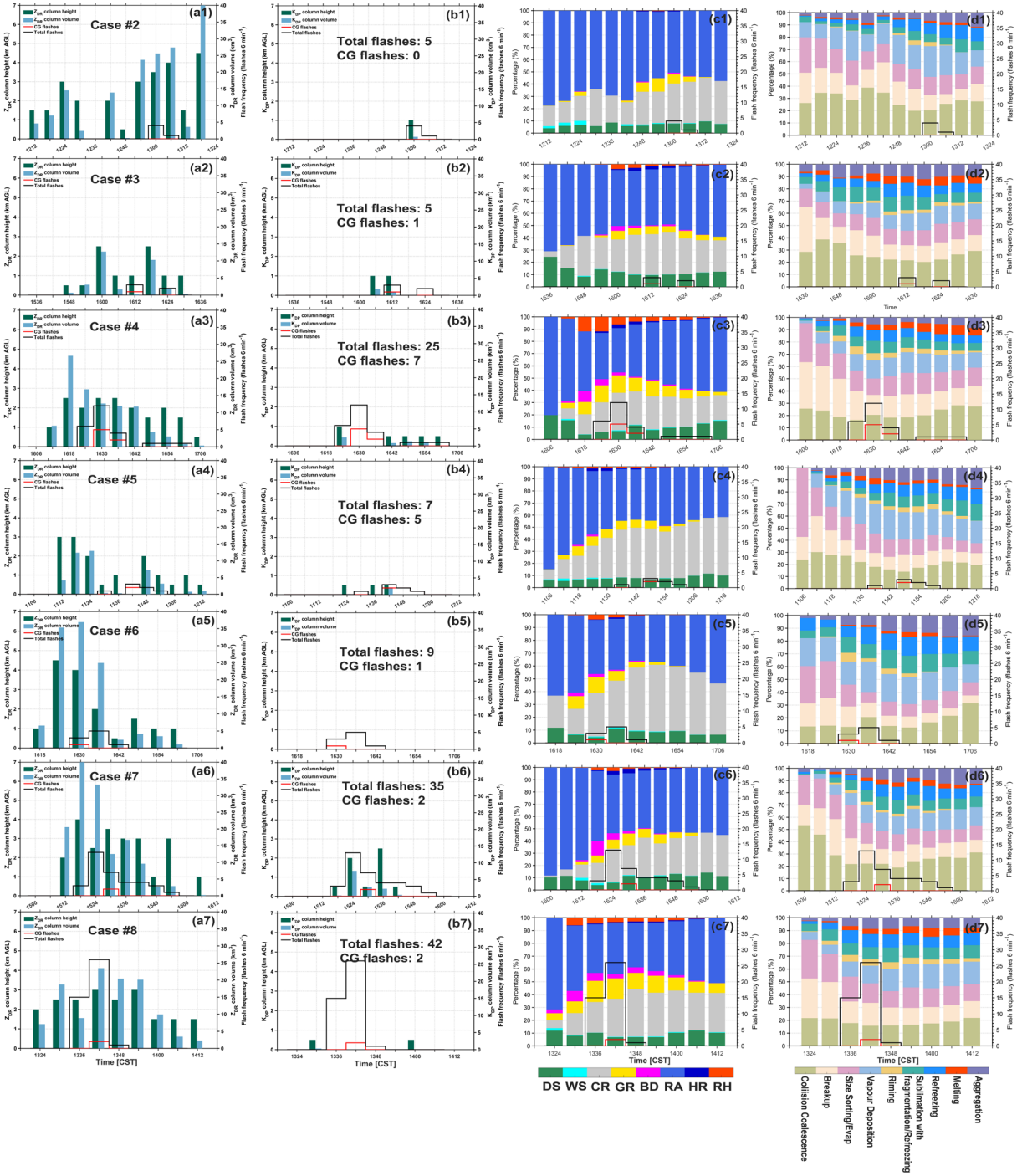

Figure 10. The variation in Z_{DR} column height and volume with the life cycle of thunderstorms (cases #2 to #8) (a1-a7). The variation in the K_{DP} column height and volume with the life cycle of

thunderstorms (cases #2 to #8) (b1-b7). The dark green bars indicate the column heights, and the light blue bars indicate the column volumes. The texts display the number of total flashes and CG flashes in a thunderstorm. The variation in percentages of hydrometeor types with the life cycle of thunderstorms (cases #2 to #8) (c1-c7). The variation in percentages of microphysical fingerprints with the life cycle of thunderstorms (cases #2 to #8) (d1-d7). The black stair lines indicate the total flashes, and the red stair lines indicate the CG flashes.

The results show that the percentages of identified graupel particles and riming process are closely related to lightning activities (Figures 10 c1-c7, d1-d7 and Figures 11 c1-c7, d1-d7), which are consistent with that in Figure 7. The cross-correlation approach can be used to examine the correlation considering the time lag, which is important for verifying whether a parameter is appropriate for forecasting another parameter. To further determine the correlation between lightning activity and the polarimetric structure. The cross correlations between the lightning activity and polarimetric structure during the life cycles in all the cases are examined, and the results are displayed in Figure 12.

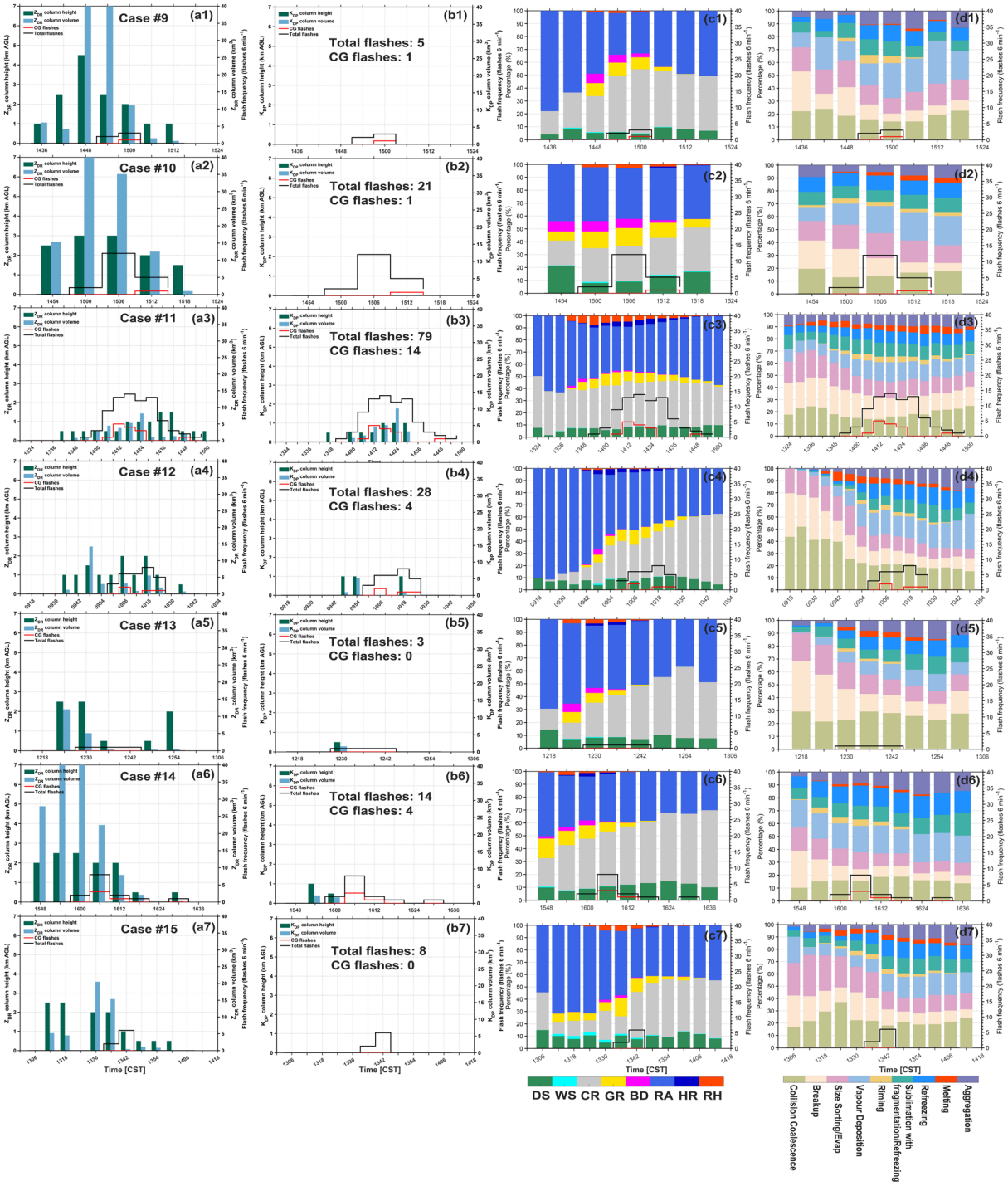

Figure 11. The variation in Z_{DR} column height and volume with the life cycle of thunderstorms (cases #9 to #15) (a1-a7). The variation in the K_{DP} column height and volume with the life cycle of thunderstorms (cases #9 to #15) (b1-b7). The dark green bars indicate the column heights, and the light blue bars indicate the column volumes. The texts display the number of total flashes and CG flashes in a thunderstorm. The variation in percentages of hydrometeor types with the life cycle of thunderstorms (cases #9 to #15) (c1-c7). The variation in percentages of microphysical

fingerprints with the life cycle of thunderstorms (cases #9 to #15) (d1-d7). The black stair lines indicate the total flashes, and the red stair lines indicate the CG flashes.

Figure 12a shows that the variation in the graupel or rain water content above the melting level within the cloud can predict the lightning activity (total flashes) after 6 minutes well, and the correlation coefficient is approximately 0.8. However, other parameters (e.g., Z_{DR} column volume, ice content above the melting level, and graupel volume) also exhibit good performance in forecasting lightning activity, and the correlation coefficient can reach approximately 0.7. The graupel volume is calculated based on the identification results of hydrometeors. Although the variation in the graupel or rain water content above the melting level within the cloud can also forecast the lightning activity (CG flashes) after 6 minutes, the correlation coefficient decreases to approximately 0.56 (Figure 12b). Notably, the trend of the Z_{DR} column volume implies that it may perform well with a longer warning time (e.g., 12 minutes) for lightning activity.

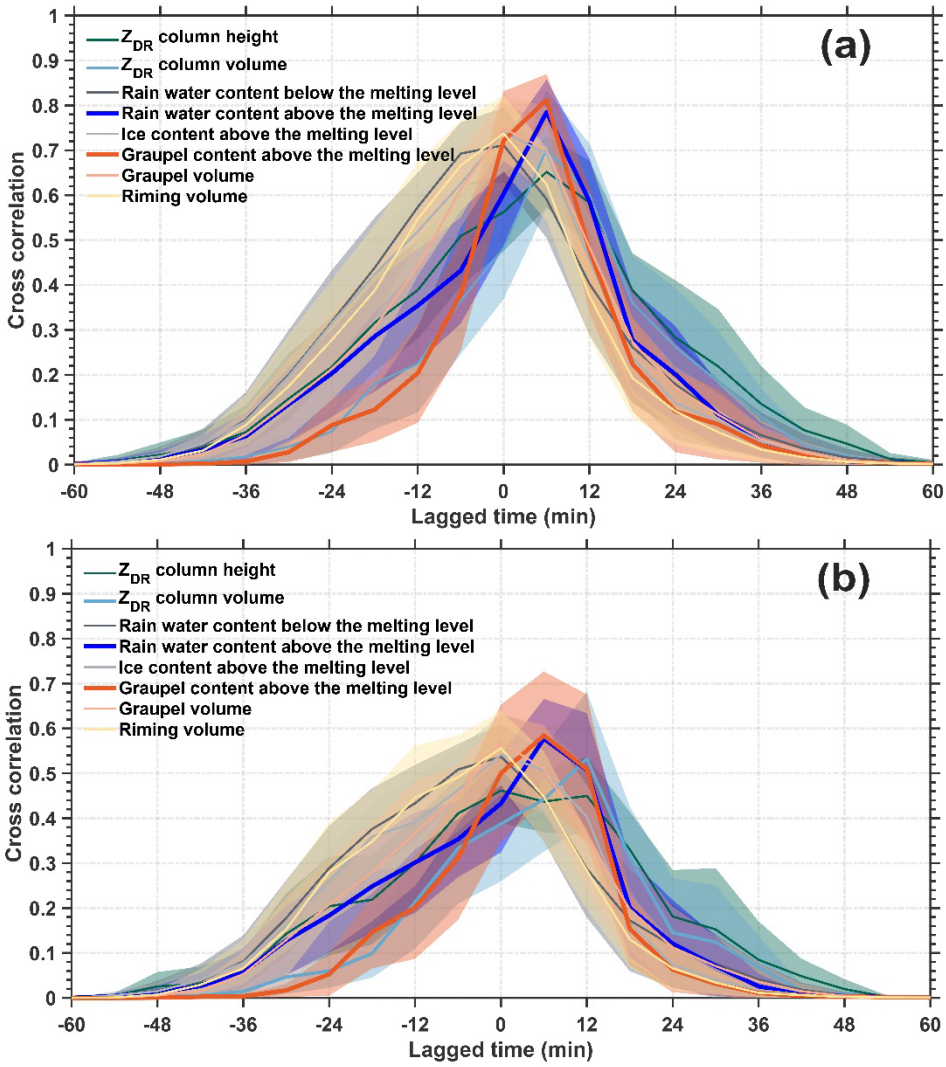

Figure 12. Cross-correlations between flash frequency (total flashes (a), CG flashes (b)) and eight radar-retrieved variables (Z_{DR} column height/volume, rain water content below/above the melting level, ice content above the melting level, graupel content above the melting level, graupel volume, and riming volume); the lines indicate the mean values and the shaded area indicates the 95% confidence interval. The lagged time is for flash frequency lags these eight radar-retrieved variables."

Lines 719−748 in mms:

"As discussed in Section 3.2, lightning activity is indeed related to dynamic variation and impulses in vertical velocity, which is consistent with the findings of previous studies (e.g., Bruning et al., 2024; Sharma et al., 2024; Sharma et al., 2021). The unsteady Z_{DR} and K_{DP} columns are tied to unsteady updrafts associated with thermal bubbles, which are relatively short-lived and thus indicate an impulse in vertical velocity. In this way, the variations in the Z_{DR} and K_{DP} columns can indicate lightning activity. Although this hypothesis is reasonable and supported by observations through the microphysical signatures of large-drop lofting and glaciation corresponding to the Z_{DR} and K_{DP} columns (Bruning et al., 2024; Fridlind et al., 2019); however, the observations of Sharma et al. (2024) and Sharma et al. (2021) revealed that the K_{DP} column volumes (or mean K_{DP} values within a segmented K_{DP} column) have noticeably different pattern than the Z_{DR} column volumes (or mean Z_{DR} values within a segmented Z_{DR} column), which has remained a question in Sharma et al. (2021).

In this study, we explore the polarimetric and microphysical structures related to impulse events and lightning activity. The results indicate that the column within the reflectivity core is only the Z_{DR} column in which the impulse event initially develops; then, the supercooled raindrops indicated by the Z_{DR} column transfer to abundant graupel and/or hailstone particles, releasing latent heat and thus invigorating convection; accompanying the Z_{DR} column within the reflectivity core, it collapses, and lightning intensifies. Moreover, the formation of the K_{DP} column requires melting and shedding processes from large ice particles (e.g., graupel or hailstones) that produce many raindrops of moderate-to-large and small sizes, which contribute to high Z_{DR}/K_{DP} values. These raindrops can recirculate into updrafts and be lifted to the mixed-phase region, forming the Z_{DR} column first, but then, it collapses as graupel and/or hailstone particles increase. Convection and lightning are enhanced, and a K_{DP} column is formed, which is associated with an increasing number of small-to-moderate hailstones with a significant water fraction. Thus, the Z_{DR} and K_{DP} columns within the reflectivity core are associated with the different stages of an impulse event, the Z_{DR} column indicates the stage in which cold cloud processes are weak, and the K_{DP} column is the opposite of

the Z_{DR} column. This may explain the remaining question in Sharma et al. (2021), namely, why the K_{DP} column has a noticeably different pattern than the Z_{DR} column does. Notably, the Z_{DR} column is located at the periphery of the reflectivity core when the Z_{DR} column collapses within the reflectivity core."

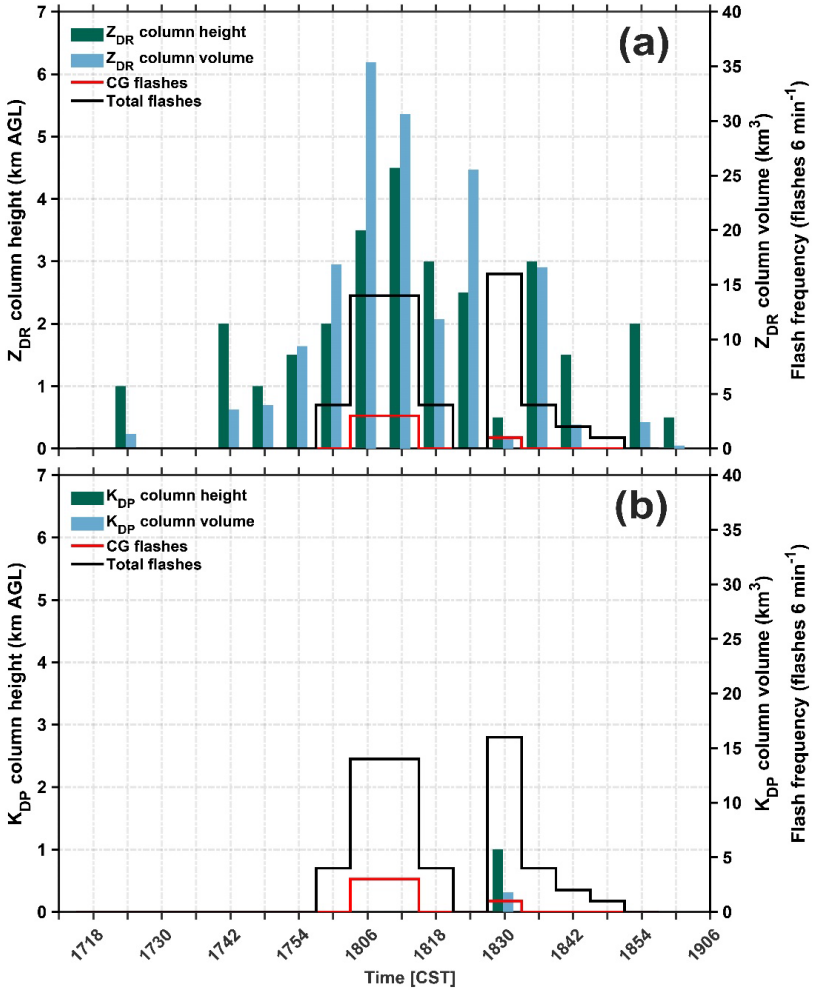

Figure 5. Time–height (volume) variation in the Z_{DR} column (a) and K_{DP} column (b). The dark green bars indicate the column heights and the light blue bars indicate the column volumes. The black (red) stepped line indicates the total flashes (CG flashes) from the LFEDA. AGL (above ground level).

Bruning, E. C., Brunner, K. N., van Lier-Walqui, M., Logan, T. and Matsui, T.: Lightning and Radar Measures of Mixed-Phase Updraft Variability in Tracked Storms during the TRACER Field Campaign in Houston, Texas. Monthly Weather Review, 152, 2753-2769, https://doi.org/10.1175/MWR-D-24-0060.1, 2024.

Fridlind, A. M., van Lier-Walqui, M., Collis, S., Giangrande, S. E., Jackson, R. C., Li, X., Matsui, T., Orville, R., Picel, M. H., Rosenfeld, D., Ryzhkov, A., Weitz, R., and Zhang, P.: Use of polarimetric radar measurements to constrain simulated convective cell evolution: a pilot study

with Lagrangian tracking. Atmospheric Measurement Techniques, 12(6), 2979-3000, https://doi.org/10.5194/amt-12-2979-2019, 2019.

Kumjian, M. R.: The Impact of Precipitation Physical Processes on the Polarimetric Radar Variables. Ph. D. Dissertation, The University of Oklahoma, Norman, OK, USA, 327p., 2012.

Kumjian, M. R., Prat, O. P., Reimel, K. J., van Lier-Walqui, M. and Morrison, H. C.: Dual-Polarization Radar Fingerprints of Precipitation Physics: A Review. Remote Sensing, 14, 3706, https://doi.org/10.3390/rs14153706, 2022.

Sharma, M., Tanamachi, R. L. and Bruning, E. C.: Investigating Temporal Characteristics of Polarimetric and Electrical Signatures in Three Severe Storms: Insights from the VORTEX-Southeast Field Campaign. Monthly Weather Review, 152(7): 1511-1536, https://doi.org/10.1175/MWR-D-23-0144.1, 2024.

Sharma, M., Tanamachi, R. L., Bruning, E. C. and Calhoun, K. M.: Polarimetric and Electrical Structure of the 19 May 2013 Edmond–Carney, Oklahoma, Tornadic Supercell. Monthly Weather Review, 149(7): 2049-2078, https://doi.org/10.1175/MWR-D-20-0280.1, 2021.

Zhao, C., Zheng, D., Zhang, Y. J., Liu, X., Zhang, Y., Yao, W., and Zhang, W.: Characteristics of cloud microphysics at positions with flash initiations and channels in convection and stratiform areas of two squall lines, Journal of Tropical Meteorology, 37: 358-369, doi:10.16032/j.issn.1004-4965.2021.035, 2021b.

2) *355-57: It is not clear to me that the Zh signal is better related to lightning. – for instance, the Zh signal is quite noisy, while there is a very clear max in high LWC values just before each of the peaks in lightning that is much less noisy – and the authors conclude later that the LWC signal is the most robust. So this claim confused me.*

Reply: Thank you for your careful review. This description is indeed confusing. We have deleted the confusing description ("However, the relationship between the liquid water content within the Z_{DR} columns and the lightning flash frequency is not as strong as that between the Z_H values within the Z_{DR} columns and the lightning flash frequency"). Please see in mms (Lines 524−527).

3) *369: how does the collapse of the column result in an increase in lightning if graupel (which is thought to be necessary for electrification) is inferred as decreasing or absent in the column? Further discussion of the process would be valuable here; there are some hints in the discussion/conclusion section here, but I felt that further information and data was needed to verify the interpretation of the two different pathways to lightning the authors have identified.*

Reply: Yes. We agree with your insightful comment and suggestion. We have added the related analysis and discussion in **Section 3.2**. Please see in mms (Lines 451−508).

Lines 451−508 in mms:

"**3.2 Vertical structures of microphysics related to lightning activity**

To study the vertical thunderstorm structure related to lightning activity, we explore the vertical structures of polarimetric radar variables and microphysics, in combination with 3D lightning location data. Figure 7 displays the cross sections of polarimetric radar variables (Z_H, Z_{DR}, and K_{DP}) and microphysics (hydrometeor types and microphysical fingerprints) from the Cartesian grid of the studied isolated thunderstorm. At 18:00 CST (Figure 7 a1-e1), the lightning activity begins, and the locations of the flash sources are high and correspond mainly to graupel particles. Riming occurrence surrounds the flash sources. The Z_{DR} column and reflectivity core (≥ 40 dBZ) begin to separate, having previously been overlapping during the initial development stage of the thunderstorm (Figure 4a, b). Then, at 18:06 CST (Figure 7 a2-e2), riming begins obviously, the echoes strengthen (≥ 55 dBZ), and the heights of the strong echoes are lifted. This finding indicates that the convective strength or updrafts are obviously increased and that the cold cloud processes are heavily. The lightning activity reached the first peak, where the locations of the flash sources mainly corresponded to graupel and ice particles. Moreover, the Z_{DR} column is located at the periphery of the reflectivity core, and high K_{DP} values occur and correspond to heavy rain particles, which are associated with large ice particles (e.g., hailstones) melting, raindrops coalescence and/or break. This phenomenon is consistent with that the K_{DP} tends to be directly proportional to the rain mixing ratio (Snyder et al., 2017).

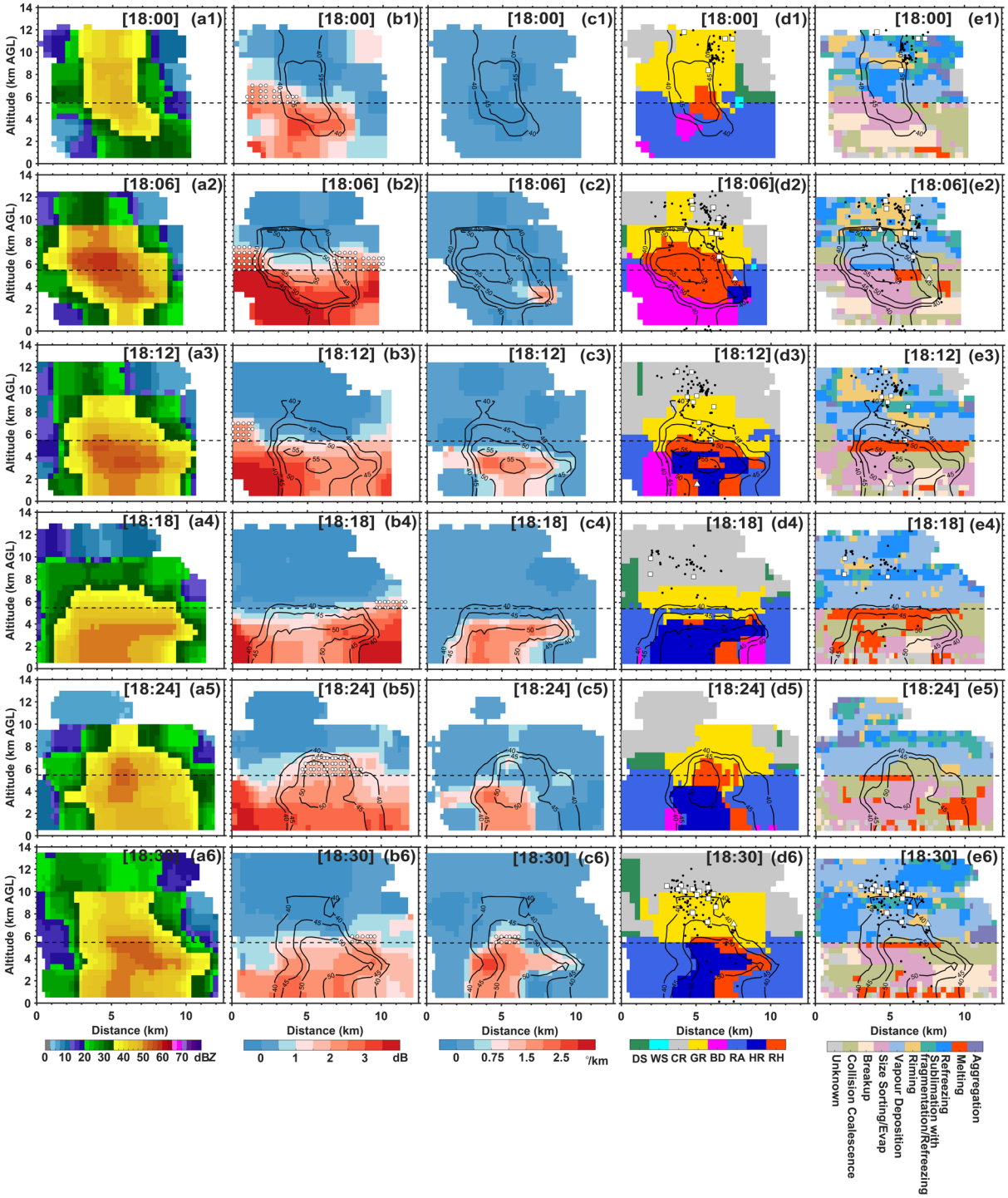

Figure 7. Cross sections of polarimetric radar variables (Z_H, Z_{DR}, and K_{DP}) and microphysics (hydrometeor types and microphysical fingerprints) from the Cartesian grid of the isolated thunderstorm (case #1). At 18:00 CST (a1-e1), 18:06 CST (a2-e2), 18:12 CST (a3-e3), 18:18 CST (a4-e4), 18:24 CST (a5-e5), and 18:30 CST (a6-e6). The black dashed line indicates the 0°C isotherm height. The white dots indicate the areas of the identified Z_{DR}/K_{DP} columns. The black contours with values indicate the reflectivity structure. The black dots indicate the flash

sources, the white square represents the first source of the intracloud flash, and the triangle represents the CG flash.

Subsequently, the lightning activity weakened at 18:12 and 18:18 CST. During this stage (Figure 7 a3-e3, a4-e4), the reflectivity core is landing and large ice particles above the melting level decrease, corresponding to heavy melting and indicating increasing downdrafts. Although Z_{DR} columns are present, they can only indicate updrafts around the reflectivity core. However, the reflectivity core was lifted again at 18:24 CST (Figure 7 a5). The contents of rain and hail mixtures and graupel clearly increased (Figure 7 d5). This indicates that the convective strength or updrafts are increased. Notably, the Z_{DR} column and reflectivity core overlap again, just as occurred during the initial development of the thunderstorm (Figure 4a, b; Figure 7 b5). Although a few high K_{DP} values occurred above the melting level, a K_{DP} column formed during the next 6 minutes (Figure 7 c5, c6). At 18:30 CST (Figure 7 a6-e6), the lightning activity reaches the second peak, and the riming process surrounds these flash sources. The Z_{DR} column within the reflectivity core quickly collapses with the occurrence of abundant graupel particles.

In total, this thunderstorm shows two impulses in vertical velocity, which correspond to two lightning activity peaks. When the first impulse event initially develops, the Z_{DR} column is obvious and overlaps with the reflectivity core; however, the region of the Z_{DR} column within the reflectivity core will collapse, with abundant graupel particles forming by riming or freezing, stimulating updrafts and intensified lightning. When large ice particles (e.g., graupel or hailstone) subsequently decrease, indicating the end of the first impulse event, melting and shedding processes occur, resulting in more raindrops (many moderate-to-large and small raindrops) contributing to high Z_{DR}/K_{DP} values. These raindrops could recirculate into the updrafts and be lifted to the mixed-phase region, forming the Z_{DR} column first, and raindrops could transfer to abundant graupel and even hailstones, releasing latent heat and thus invigorating updrafts again (indicating the second impulse event). However, the Z_{DR} column within the reflectivity core will collapse with increasing amounts of graupel and/or hailstone particles, but the K_{DP} column will occur; this can be explained by the increased K_{DP} values at the column top being associated with an increasing number of small-to-moderate hailstones with significant water fractions (Snyder et al., 2017). The lightning activity also reaches a peak value.

Thus, the Z_{DR} column within the reflectivity core is likely an indicator of imminent convection invigoration via latent heat release and then the formation of abundant graupel particles promotes lightning activity via noninductive charging; the K_{DR} column

is highly related to cold cloud processes, replacing Z_{DR} column to indicate updrafts within the reflectivity core when obvious graupels and hailstones occur."

4) *393: note, however, that the correlation with Zdr is relatively large and increases (0.6) for about 20 min before the maximum in lightning, but falls off rapidly by 12 min after the lightning increases. From a practical point of view, the timing of the maximum correlation is less important than a trend toward confidence for lightning, and so in that sense the Zdr signal is more helpful.*

Reply: Yes, we agree with your opinion. Now, we added more cases (fifteen cases in total) to present the statistical results in **Section 3.4**, replacing the results of a case study in the raw manuscript. Moreover, we conclude and discuss the results in **Section 4**. Please see in mms (Lines 624−639; Lines 762−808).

Lines 624−639 in mms:

"Figure 12a shows that the variation in the graupel or rain water content above the melting level within the cloud can predict the lightning activity (total flashes) after 6 minutes well, and the correlation coefficient is approximately 0.8. However, other parameters (e.g., Z_{DR} column volume, ice content above the melting level, and graupel volume) also exhibit good performance in forecasting lightning activity, and the correlation coefficient can reach approximately 0.7. The graupel volume is calculated based on the identification results of hydrometeors. Although the variation in the graupel or rain water content above the melting level within the cloud can also forecast the lightning activity (CG flashes) after 6 minutes, the correlation coefficient decreases to approximately 0.56 (Figure 12b). Notably, the trend of the Z_{DR} column volume implies that it may perform well with a longer warning time (e.g., 12 minutes) for lightning activity.

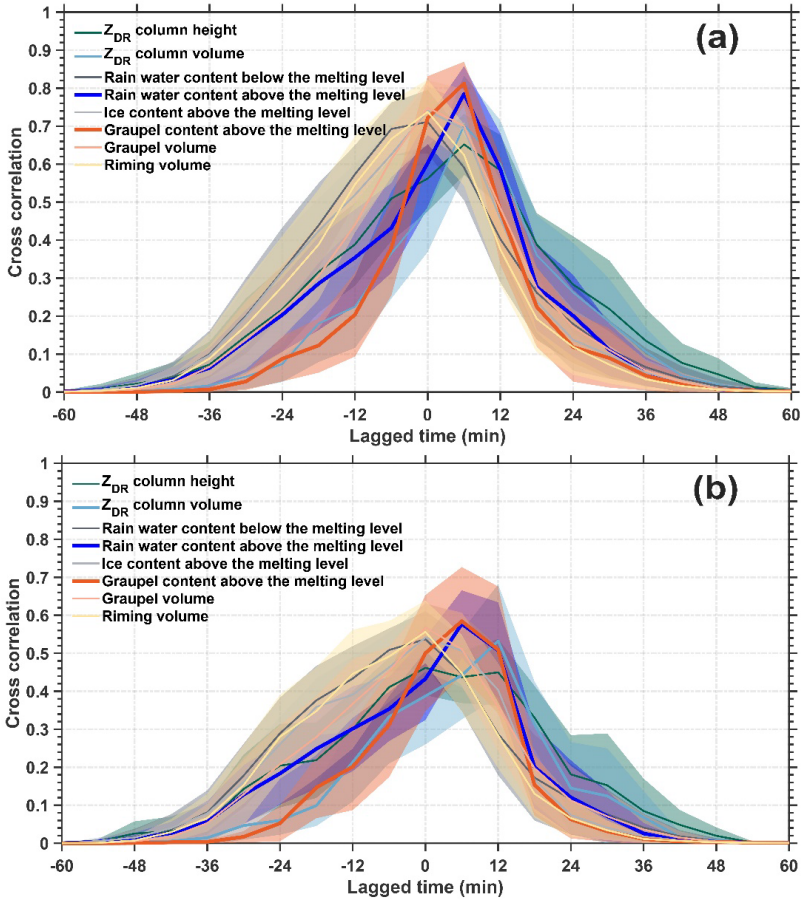

Figure 12. Cross-correlations between flash frequency (total flashes (a), CG flashes (b)) and eight radar-retrieved variables (Z_{DR} column height/volume, rain water content below/above the melting level, ice content above the melting level, graupel content above the melting level, graupel volume, and riming volume); the lines indicate the mean values and the shaded area indicates the 95% confidence interval. The lagged time is for flash frequency lags these eight radar-retrieved variables."

Lines 762−808 in mms:

"We bridged the polarimetric structure (the Z_{DR}/K_{DP} column, supercooled liquid water, and graupel content below 0°C) and lightning activity on the basis of observations of fifteen isolated thunderstorm cells (the variation curve is conceptualized in Figure 13). The two peaks of lightning activity in Figure 13 suggest multiple impulse events in convection; specifically, the first peak refers specifically to the initial impulse event, but the second peak suggests subsequent impulse events. The magnitude of the amplitudes among these curves has no practical meaning; it is merely for visualization purposes.

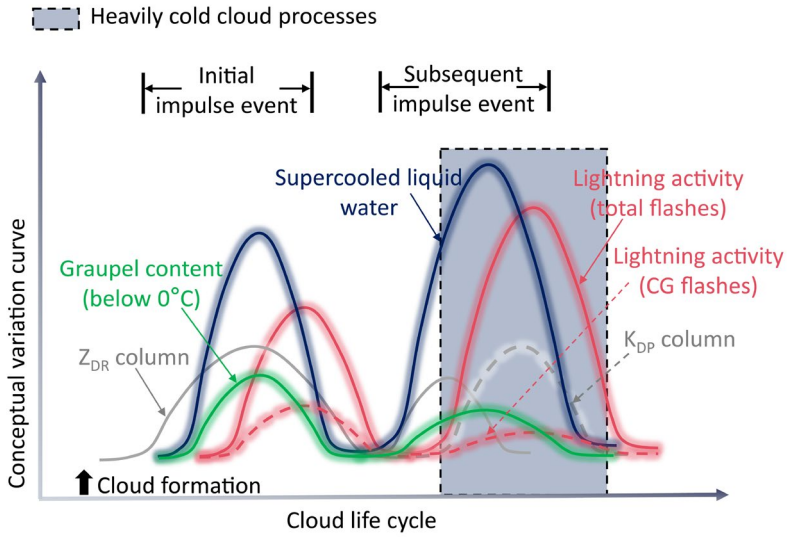

Figure 13. A conceptual model bridging the polarimetric structure and lightning activity.

In our opinion (Figure 13), the Z_{DR} column within the reflectivity core is likely an indicator of imminent convection invigoration via latent heat release, after which the formation of abundant graupel particles promotes lightning activity via noninductive charging. Therefore, microphysics (e.g., graupel content) are more directly related to lightning activity than are dynamics (e.g., the Z_{DR} column). Moreover, the observations reveal that the microphysical variations in supercooled liquid water and graupel yield better correlation coefficients for the prediction of lightning activity at short warning times (e.g., 6 minutes in this study) than do the dynamical variations in the Z_{DR} column volume. However, the trend of the Z_{DR} column volume implies that it may perform well with a longer warning time (e.g., 12 minutes in this study) for lightning activity. The K_{DR} column is highly related to cold cloud processes. Thus, the K_{DP} column is likely absent when the impulse event initially develops; however, it will be present later with heavily cold cloud processes, replacing the Z_{DR} column to indicate updrafts within the reflectivity core when obvious graupels and hailstones are occurring. In addition, the 6-min or 12-min warning time in our results is likely due to the temporal resolution (6 minutes) of the radar data used in this study; high temporal resolution observations of phased-array radar may decrease the uncertainty.

Notably, the threshold value for identifying the Z_{DR} column (≥1.5 dB) in this study is different from that (≥1 dB) in previous studies (e.g., Sharma et al., 2024). Although this threshold value is selected according to the retrieved raindrop diameter, which should exceed 2 mm within the Z_{DR} column during the initial phase of a storm (Kumjian, et al., 2014), the results for quantifying the Z_{DR} column (i.e., height and volume) may be different from those of previous studies that used the 1 dB threshold (e.g., Sharma et al., 2024). However, this study focuses on the trend of the Z_{DR} column height or

volume; thus, the differences resulting from different thresholds are relieved. The threshold value for identifying the K_{DP} column (≥1°/km) in this study is consistent with that used by Sharma et al. (2024). However, the different estimation methods for K_{DP} may introduce additional uncertainty, as discussed in Sharma et al. (2021).

Moreover, the height of the melting layer (0°C), which is derived from environmental soundings, is assumed to be constant for identifying and quantifying the Z_{DR}/ K_{DP} column; however, the melting level is frequently elevated within updraft cores because of latent heat release, which is influenced by the strength of updrafts relative to the ambient environment. Thus, a more accurate melting level will decrease the biased estimations of the "3D mapping columns" method in this study. In addition, although our results support some observations in Bruning et al. (2024) and seem to explain the remaining question in Sharma et al. (2024) and Sharma et al. (2021), whether there are differences between such small, isolated, subtropical thunderstorms and other thunderstorm types (i.e., mesoscale convective systems, supercells, or tropical thunderstorms) should be further analysed to reduce the probability of uncertainty in our study. Finally, although the results retrieved from hydrometeor identification and microphysical fingerprint methods are reasonable and obey theoretical cognition in this study, the potentially biased estimates may result from isothermal height and the status of the hydrometeor (e.g., canting angle)."

5) *423-6: These correlation coefficients do not seem different enough to allow the authors to say one is best, especially on the basis of a single case study. Values all >0.8 are quite high for each of these variables.*

Reply: Thank you for your comment. We absolutely agree with your suggestion. We have corrected all of these descriptions. In addition, more cases have been added to strengthen our results. Please see in mms (Lines 624−639; Lines 762−808). The related content has already been presented in the last reply.

6) *449: After studying the lead times and identifying and emphasizing a 6 min lead time in their results section, the authors return to quoting the 36 min lead time in their conclusions, which does not seem supported by the detailed analysis the authors undertook. Of course, the 36 min lead is there in the data, but it is not well-correlated to lightning. Many moderately vigorous storms will produce a small Zdr column without going on to produce lightning. Likewise on 476-477, I would be reluctant to forecast lightning on the basis of a 36 min lead - that cell is simply one to keep an eye on for future lightning.*

Reply: Yes. This description is unreasonable; we have deleted the related content and corrected this opinion on the basis of the statistical results. Please see in mms (Lines 624−639; Lines 762−808). The related content has already been presented in your 4th comment.

7) *Fig. 12: the authors indicate that no Kdp column was present in their data, but do not show Kdp in Fig. 6. I would like to see further data on this, as it may explain the relatively fewer cases in Bruning et al. (2024) that had Zdr columns and lightning but did not have a Kdp column.*

Reply: Yes, more information about the K_{DP} column is helpful for comparing the results of this study with those of other studies (e.g., Bruning et al., 2024). Now, we have presented more information about the K_{DP} column in context (Figure 5). Our results indeed support the observations of Bruning et al. (2024). Please see in mms (Lines 586−597).

Lines 586−597 in mms:

"The variations in the Z_{DR}/K_{DP} column height and volume with the life cycle of the remaining fourteen cases are displayed in Figures 10 (cases #2 to #8) and 11 (cases #9 to #15), as are the variations in the percentages of hydrometeor types and microphysical fingerprints. The grid is assigned to specific particle type based on the results of hydrometeor identification, and the percentage of grids for each hydrometeor type is calculated. Similarly, this process is applied to determine the percentage of grids associated with microphysical fingerprints. Each of them has a Z_{DR} column (Figure 10 a1-a7, Figure 11 a1-a7); however, the absence of a K_{DP} column is possible (Figures 10 b1-b7, Figures 11 b1-b7). The results of our study support the observations of Bruning et al. (2024), namely, lightning is not observed in the absence of a Z_{DR} column, and a K_{DP} column is not observed without a Z_{DR} column. Moreover, the highest lightning flash frequency (in case #11) is observed when the Z_{DR} and K_{DP} columns are co-present, which is consistent with the observations of Bruning et al. (2024). In addition, our results suggest that the signal in the K_{DP} column within these small, isolated, subtropical thunderstorms over South China is not as steady as that in the Z_{DR} column during the life cycle."

Minor comments

1) *31: The grammar implies lightning flashes can be detected with polarimetric structures; this is not directly possible. The polarimetric signatures are proxies for lightning with some associated error. Please rephrase.*

Reply: Corrected. Please see in mms (Lines 31−32).

Lines 31−32 in mms:

"Polarimetric structures detected by radar can characterize cloud microphysics and dynamics."

2) *37: "establish" — this study is not the first to use this method, as many of the authors' citations show. "Build on" or "improve" would be a better choice, since "establish" implies that the authors have made a pioneering advancement. There are some thoughtful adjustments to past methods here, but they are incremental refinements.*

Reply: Corrected. "establish" → "improve". Please see in mms (Line 38).

3) *124: "later" - do the authors mean a time scale immediately following the Zdr column (~5 min) or subsequent updraft pulses in a multicellular sequence (~20-30 min per cell)?*

Reply: We have corrected this confusing sentence. Please see in mms (Lines 136−138).

Lines 136−138 in mms:

"Thus, the formation of a K_{DP} column is tied to cold cloud microphysics, which usually lag behind the appearance of the Z_{DR} column."

4) *125: "attempted to determine the constraints of" should be "attempted to constrain"*

Reply: The draft has been revised as suggested. Please see in mms (Line 139).

5) *140-141: "therefore the correlation coefficient … was not high." What does "therefore" mean here? It typically indicates that a conclusion has been reached, so the facts supporting the conclusion need to be stated first. They seem to be in the sentence following "therefore".*

Reply: Yes, this word is inappropriate here. We have revised the related content. Please see in mms (Lines 150−167).

Lines 150−167 in mms:

"Sharma et al. (2024) conducted a study on the basis of hypotheses, namely, that the deeper and wider the Z_{DR} and K_{DP} columns were in cases with robust and wide updrafts (e.g., Homeyer and Kumjian, 2015; Snyder, et al., 2017), the more an increase in the volumes of the Z_{DR} and K_{DP} columns would correspond to an increase the mixed-phase ice mass flux, resulting in an increase in the total flash rate; the correlation coefficient (−0.47~0.37 for the Z_{DR} column; 0.54~0.74 for the K_{DP} column) between Z_{DR} or K_{DP} columns and lightning activity was not as high as the microphysical parameters explored in previous studies (e.g., Carey and Rutledge 2000). Moreover, the results seem to be inconsistent with those of Sharma et al. (2021), who reported that the variability in flash rates is best explained by fluctuations in the Z_{DR} column volume, with a high correlation coefficient value (0.72). One possible explanation is that the effect of the time lag may decrease this correlation coefficient. As reported by Carey and Rutledge (2000), they obtained a very high one-lag (7 minutes) correlation coefficient (ρ = 0.9) between the graupel mass within the mixed-phase zone and the CG lightning flash rate, suggesting that the directly related microphysics with noninductive charging have a greater correlation coefficient with lightning activity. Another possible way is that the interactions of the Z_{DR}/K_{DP} column with dynamics and microphysics are uncertain, which affects the results under the current hypotheses. This is also emphasized in Sharma et al. (2021) and raised as a retained question in the appendix. Thus, further exploration is needed."

6) *175-181: what Kdp calculation method was used? Kdp is a very noisy measurement, and so is very sensitive to algorithm design and configuration choices.*

Reply: Yes, the K_{DP} calculation method must be displayed. We have added this information. Please see in mms (Lines 214−218).

Lines 214−218 in mms:

"We utilized two methods to smooth the differential phase Φ_{DP}, namely, "lightly filtering" (2-km) and "heavily filtering" (6-km), as in Park et al. (2009). Two estimates of K_{DP} were subsequently obtained from a slope of a least squares fit of the filtered Φ_{DP}; a lightly filtered K_{DP} was subsequently used in the case of horizontal reflectivity > 40 dBZ, and a heavily filtered K_{DP} was selected otherwise (Ryzhkov and Zrnić, 1996)."

Park, H. S., Ryzhkov, A. V., Zrnić, D. S., and Kim, K.: The Hydrometeor Classification Algorithm for the Polarimetric WSR-88D: Description and Application to an MCS. Weather and Forecasting, 24: 730-748, https://doi.org/10.1175/2008WAF2222205.1, 2009.

Ryzhkov, A., and Zrnić, D.: Assessment of Rainfall Measurement That Uses Specific Differential Phase. Journal of Applied Meteorology and Climatology, 35: 2080-2090, https://doi.org/10.1175/1520-0450(1996)035<2080:AORMTU>2.0.CO;2, 1996.

7) *220: here and throughout the paper, melting level is preferable, since melting always begins at this level for any hydrometeor but freezing might not.*

Reply: Thanks for the suggestion. The draft has been revised as suggested.

8) *221: What are other parameters (CAPE, etc.) of this sounding? They would be helpful in placing this storm in the context of other environments globally.*

Reply: The CAPE values of these thudnerstorms are provided in Table 1.

9) *227: "automatically" should be "automatic"*

Reply: Corrected.

10) *271: A new sentence should start after "(Figure 2e,f)".*

Reply: Corrected.

11) *281: "resulted by" should be "resulting from"*

Reply: Corrected.

12) *447: I suggest dropping "inappropriate". Any algorithm choice requires some judgment, and reflectivity thresholds have a sound physical basis and are in wide use. Of course, using fewer or improved variables and thresholds is also good, and in that way the authors have made a nice methodological contribution, but "inappropriate" is unnecessarily harsh.*

Reply: Thanks very much for this suggestion. The draft has been revised as suggested. Please see in mms (Line 694).

Line 694 in mms:

"…avoiding the utilization threshold value of Z_H."

Referee #2 Evaluations:

General Comments:

The authors investigated the relationships between polarimetric radar signatures (ZDR and KDP columns) and lightning activity throughout the lifecycle of an isolated

thunderstorm. The authors present a methodology using a "3D mapping columns" approach to analyze radar data in detail. They found that the content of supercooled rainwater/graupel is the most relevant parameter to total flashes/cloud-to-ground flashes. Overall, the manuscript is well structured and easy to follow. However, there are several sections that require clarification and elaboration. The authors need to mention caveats/limitations of using "3D mapping columns" more effectively. Microphysics analysis is weak and lacks justifications for many of their observations. A more conservative approach can be adopted, which is to recommend monitoring parameters such as volume and variations of ZH intensity within ZDR columns, and supercooled liquid water content as a proxy for potential lightning activity development instead of using the term "forecast." The recommendation is that the manuscript should be reconsidered after major revisions.

We appreciate your professional evaluation and valuable comments. These careful suggestions and constructive comments helped us improve this manuscript.

Specific comments:

1. The analysis is based on a single isolated thunderstorm. While this allows detailed examination, it raises questions about the universality of the conclusions. The authors should include enough cases to obtain robust statistical relationships. It is probable that the 6-min lead time might be just due to the temporal resolution (6 min) of radar data used in this study.

Reply: We absolutely agree with your suggestion that enough cases should be included to obtain robust statistical relationships. Now, more cases have been added to strengthen our results (Table 1, including the original analysis case (case #1) in the manuscript). The statistical relationships between the polarimetric radar variables and lightning activity are shown in Figure 12, **Section 3.4**. Please see in mms (Lines 624−639).

Yes, the probability that the 6-min lead time might be just due to the temporal resolution (6 min) of the radar data used in this study. We state this in **Section 4**. Please see in mms (Lines 783−785).

Table 1. The information of cases

Cases number	Time information [CST]	CAPE [J kg^{-1}]
#1	17:18 to 19:00, 20 June 2016	1277
#2	12:12 to 13:18, 26 June 2016	1225
#3	15:36 to 16:36, 3 July 2016	961
#4	16:06 to 17:06, 5 July 2016	412
#5	11:00 to 12:12, 6 July 2016	1202
#6	16:18 to 17:06, 6 July 2016	1202

#7	15:00 to 16:06, 16 July 2016	1425
#8	13:24 to 14:12, 27 July 2016	1203
#9	14:36 to 15:18, 27 July 2016	1376
#10	14:54 to 15:18, 27 July 2016	1286
#11	13:24 to 15:00, 29 May 2016	1339
#12	09:18 to 10:48, 18 June 2016	1437
#13	12:18 to 13:00, 18 June 2016	1375
#14	15:48 to 16:36, 18 June 2016	1475
#15	13:06 to 14:12, 7 July 2016	2537

Lines 624−639 in mms:

"Figure 12a shows that the variation in the graupel or rain water content above the melting level within the cloud can predict the lightning activity (total flashes) after 6 minutes well, and the correlation coefficient is approximately 0.8. However, other parameters (e.g., Z_{DR} column volume, ice content above the melting level, and graupel volume) also exhibit good performance in forecasting lightning activity, and the correlation coefficient can reach approximately 0.7. The graupel volume is calculated based on the identification results of hydrometeors. Although the variation in the graupel or rain water content above the melting level within the cloud can also forecast the lightning activity (CG flashes) after 6 minutes, the correlation coefficient decreases to approximately 0.56 (Figure 12b). Notably, the trend of the Z_{DR} column volume implies that it may perform well with a longer warning time (e.g., 12 minutes) for lightning activity.

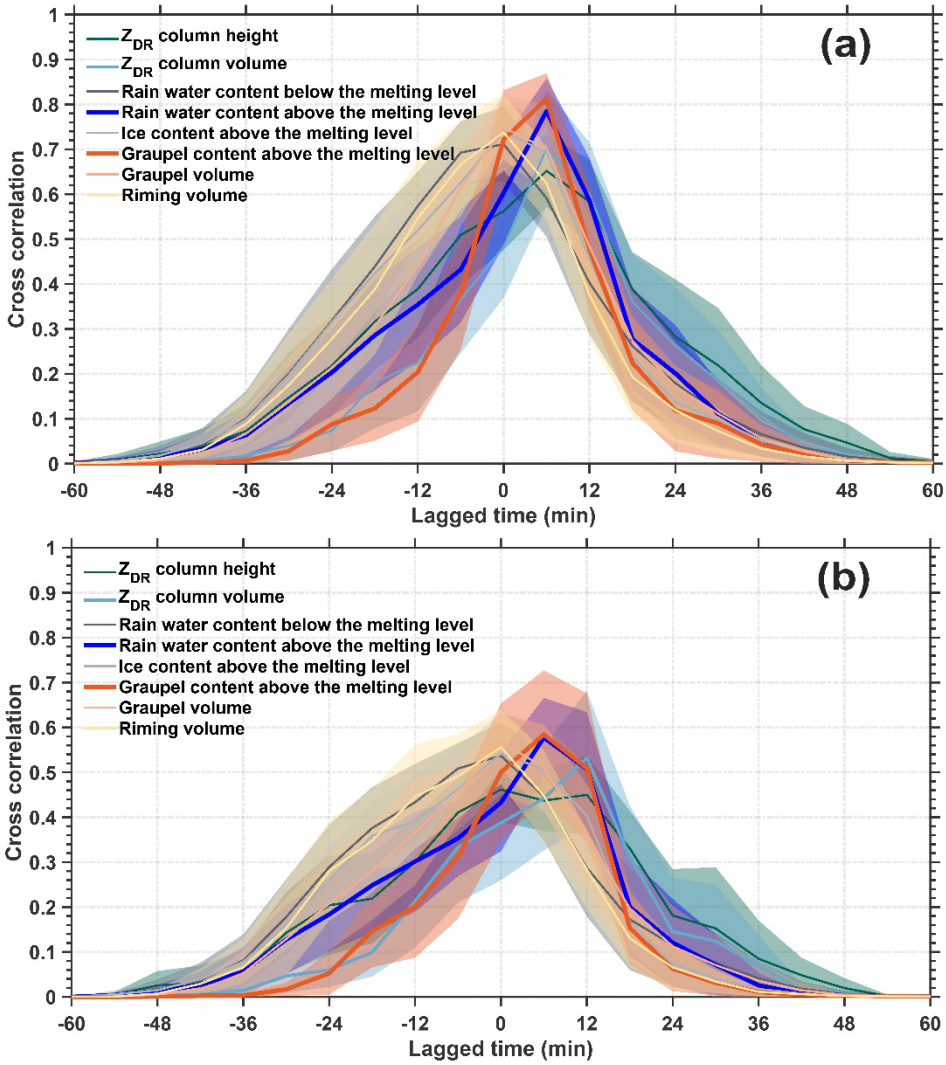

Figure 12. Cross-correlations between flash frequency (total flashes (a), CG flashes (b)) and eight radar-retrieved variables (Z_{DR} column height/volume, rain water content below/above the melting level, ice content above the melting level, graupel content above the melting level, graupel volume, and riming volume); the lines indicate the mean values and the shaded area indicates the 95% confidence interval. The lagged time is for flash frequency lags these eight radar-retrieved variables."

Lines 783−785 in mms:

"In addition, the 6-min or 12-min warning time in our results is likely due to the temporal resolution (6 minutes) of the radar data used in this study; high temporal resolution observations of phased-array radar may decrease the uncertainty."

2. The reported 36-minute lead time is also questionable due to several reasons. Firstly, it is based solely on a single case in this study. Secondly, as mentioned in the abstract

(line 42), the authors state that the initial appearance of the ZDR column can be used to forecast lightning initiation in advance. Furthermore, the authors report at least 36 minutes of lead time (line 448) for forecasting the first lightning flash (line 449) in the observed cell. This is based on the very first appearance of the ZDR column at 17:24 CST and the onset of lightning activity at 18:00 CST. Now, considering Figure 7, where each column represents an observed ZDR column, there is a gap of 12 minutes at 17:30 CST and 17:36 CST when no ZDR column was detected. Notably, the manuscript does not provide an explanation for why (17:24 CST) was chosen over the first persistent ZDR observation at 17:42 CST to report the lead time, despite the 12-minute time gap. This explanation is crucial because the reported lead time is significantly larger compared to 4~6 minutes in previous studies (referenced in line 450).

Reply: Yes. We absolutely agree with your comment. This description is unreasonable; we have deleted the related content (Lines 697−701) and corrected this opinion on the basis of the statistical results. The **Abstract** has been corrected. Please see in mms (Lines 31−50; Lines 762−785).

Lines 31−50 in mms:

"Polarimetric structures detected by radar can characterize cloud microphysics and dynamics. Many studies have indicated that differential reflectivity (Z_{DR}) and specific differential phase (K_{DP}) columns, which serve as proxies for updraft strength, are related to lightning activity; moreover, the quantities of ice and supercooled liquid water strongly influence the occurrence of lightning flashes via noninductive charging. However, the sequence or interactions among these factors with dynamics and microphysics from the perspective of the cloud life cycle are uncertain. Here, we improve the '3D mapping columns' method to identify and quantify the Z_{DR}/K_{DP} columns, which is based on Cartesian grid datasets; this method is sensitive in the early phase of cloud formation. Our study bridges the polarimetric structure and lightning activity within fifteen isolated thunderstorms during the cloud life cycle. The results indicate that microphysical variations in supercooled liquid water and graupel yield better correlation coefficients for the lightning activity prediction at short warning times (e.g., 6 minutes) than dynamical variations in the Z_{DR} column volume do; however, the trend of the Z_{DR} column volume implies good performance at longer warning times (e.g., 12 minutes). The K_{DP} column is likely absent in the early phase of convection development; however, it will occur in the later stage with heavily cold cloud processes, replacing the Z_{DR} column to indicate updrafts within the reflectivity core when obvious graupels and hailstones occur. Our study improves the understanding

of the polarimetric structure, which is related to dynamics and microphysics, and is also associated with lightning activity."

Lines 762−785 in mms:

"We bridged the polarimetric structure (the Z_{DR}/K_{DP} column, supercooled liquid water, and graupel content below 0°C) and lightning activity on the basis of observations of fifteen isolated thunderstorm cells (the variation curve is conceptualized in Figure 13). The two peaks of lightning activity in Figure 13 suggest multiple impulse events in convection; specifically, the first peak refers specifically to the initial impulse event, but the second peak suggests subsequent impulse events. The magnitude of the amplitudes among these curves has no practical meaning; it is merely for visualization purposes.

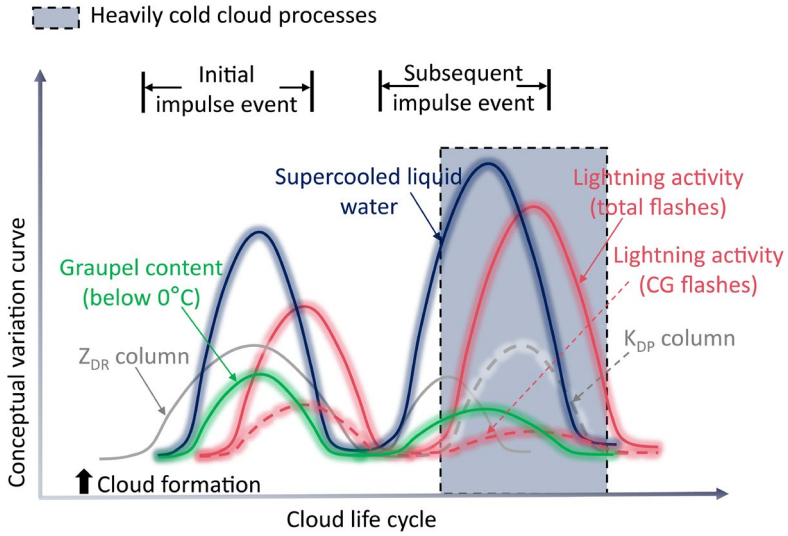

Figure 13. A conceptual model bridging the polarimetric structure and lightning activity.

In our opinion (Figure 13), the Z_{DR} column within the reflectivity core is likely an indicator of imminent convection invigoration via latent heat release, after which the formation of abundant graupel particles promotes lightning activity via noninductive charging. Therefore, microphysics (e.g., graupel content) are more directly related to lightning activity than are dynamics (e.g., the Z_{DR} column). Moreover, the observations reveal that the microphysical variations in supercooled liquid water and graupel yield better correlation coefficients for the prediction of lightning activity at short warning times (e.g., 6 minutes in this study) than do the dynamical variations in the Z_{DR} column volume. However, the trend of the Z_{DR} column volume implies that it may perform well with a longer warning time (e.g., 12 minutes in this study) for lightning activity. The K_{DR} column is highly related to cold cloud processes. Thus, the K_{DP} column is likely absent

when the impulse event initially develops; however, it will be present later with heavily cold cloud processes, replacing the Z_{DR} column to indicate updrafts within the reflectivity core when obvious graupels and hailstones are occurring. In addition, the 6-min or 12-min warning time in our results is likely due to the temporal resolution (6 minutes) of the radar data used in this study; high temporal resolution observations of phased-array radar may decrease the uncertainty."

3. The authors should discuss whether the uncertainties of retrieval methods, ZDR and KDP thresholds used in the study, spatial and temporal resolution of the radar data, etc. influence the robustness of the conclusions.

Reply: Yes. Thank you for your constructive suggestions. We added a related discussion in **Section 4**. The limitations and uncertainties of the methods and data are discussed. Please see in mms (Lines 783−808). The results of this study are compared with those of previous studies (e.g., Bruning et al. 2024; Sharma et al., 2024; Sharma et al., 2021), strengthening the robustness of the conclusions. Please see in mms (Lines 586−597; 694−704; 719−748).

Lines 783−808 in mms:

"In addition, the 6-min or 12-min warning time in our results is likely due to the temporal resolution (6 minutes) of the radar data used in this study; high temporal resolution observations of phased-array radar may decrease the uncertainty.

Notably, the threshold value for identifying the Z_{DR} column (≥1.5 dB) in this study is different from that (≥1 dB) in previous studies (e.g., Sharma et al., 2024). Although this threshold value is selected according to the retrieved raindrop diameter, which should exceed 2 mm within the Z_{DR} column during the initial phase of a storm (Kumjian, et al., 2014), the results for quantifying the Z_{DR} column (i.e., height and volume) may be different from those of previous studies that used the 1 dB threshold (e.g., Sharma et al., 2024). However, this study focuses on the trend of the Z_{DR} column height or volume; thus, the differences resulting from different thresholds are relieved. The threshold value for identifying the K_{DP} column (≥1°/km) in this study is consistent with that used by Sharma et al. (2024). However, the different estimation methods for K_{DP} may introduce additional uncertainty, as discussed in Sharma et al. (2021).

Moreover, the height of the melting layer (0°C), which is derived from environmental soundings, is assumed to be constant for identifying and quantifying the Z_{DR}/ K_{DP} column; however, the melting level is frequently elevated within updraft cores because of latent heat release, which is influenced by the strength of updrafts relative to the ambient environment. Thus, a more accurate melting level will decrease the biased

estimations of the "3D mapping columns" method in this study. In addition, although our results support some observations in Bruning et al. (2024) and seem to explain the remaining question in Sharma et al. (2024) and Sharma et al. (2021), whether there are differences between such small, isolated, subtropical thunderstorms and other thunderstorm types (i.e., mesoscale convective systems, supercells, or tropical thunderstorms) should be further analysed to reduce the probability of uncertainty in our study. Finally, although the results retrieved from hydrometeor identification and microphysical fingerprint methods are reasonable and obey theoretical cognition in this study, the potentially biased estimates may result from isothermal height and the status of the hydrometeor (e.g., canting angle)."

Lines 586−597 in mms:

"The variations in the Z_{DR}/K_{DP} column height and volume with the life cycle of the remaining fourteen cases are displayed in Figures 10 (cases #2 to #8) and 11 (cases #9 to #15), as are the variations in the percentages of hydrometeor types and microphysical fingerprints. The grid is assigned to specific particle type based on the results of hydrometeor identification, and the percentage of grids for each hydrometeor type is calculated. Similarly, this process is applied to determine the percentage of grids associated with microphysical fingerprints. Each of them has a Z_{DR} column (Figure 10 a1-a7, Figure 11 a1-a7); however, the absence of a K_{DP} column is possible (Figures 10 b1-b7, Figures 11 b1-b7). The results of our study support the observations of Bruning et al. (2024), namely, lightning is not observed in the absence of a Z_{DR} column, and a K_{DP} column is not observed without a Z_{DR} column. Moreover, the highest lightning flash frequency (in case #11) is observed when the Z_{DR} and K_{DP} columns are co-present, which is consistent with the observations of Bruning et al. (2024)."

Lines 694−704 in mms:

"The volume and height of the Z_{DR} columns are quantified via the "3D mapping columns" method, and the correlation coefficient indicates that the volume of the Z_{DR} column is better for forecasting lightning activity than the column height is. In addition, both the volume and height of a Z_{DR} column have some limitations in forecasting lightning activity, except during the early phase. This phenomenon is similar to the results of Sharma et al. (2024). In their study, the correlation coefficient between the Z_{DR} column volume and total flash rate generally monotonically decreased after the initial lightning jump, and the volume of the K_{DP} columns exhibited relatively high co-variability with the total flash rate, except in the early phase. The time lag between the formation of the Z_{DR} column and that of the K_{DP} column was consistent with the results of this study,

indicating the different formation mechanisms of the Z_{DR} and K_{DP} columns described in Section 1."

Lines 719−748 in mms:

"As discussed in Section 3.2, lightning activity is indeed related to dynamic variation and impulses in vertical velocity, which is consistent with the findings of previous studies (e.g., Bruning et al., 2024; Sharma et al., 2024; Sharma et al., 2021). The unsteady Z_{DR} and K_{DP} columns are tied to unsteady updrafts associated with thermal bubbles, which are relatively short-lived and thus indicate an impulse in vertical velocity. In this way, the variations in the Z_{DR} and K_{DP} columns can indicate lightning activity. Although this hypothesis is reasonable and supported by observations through the microphysical signatures of large-drop lofting and glaciation corresponding to the Z_{DR} and K_{DP} columns (Bruning et al., 2024; Fridlind et al., 2019); however, the observations of Sharma et al. (2024) and Sharma et al. (2021) revealed that the K_{DP} column volumes (or mean K_{DP} values within a segmented K_{DP} column) have noticeably different pattern than the Z_{DR} column volumes (or mean Z_{DR} values within a segmented Z_{DR} column), which has remained a question in Sharma et al. (2021).

In this study, we explore the polarimetric and microphysical structures related to impulse events and lightning activity. The results indicate that the column within the reflectivity core is only the Z_{DR} column in which the impulse event initially develops; then, the supercooled raindrops indicated by the Z_{DR} column transfer to abundant graupel and/or hailstone particles, releasing latent heat and thus invigorating convection; accompanying the Z_{DR} column within the reflectivity core, it collapses, and lightning intensifies. Moreover, the formation of the K_{DP} column requires melting and shedding processes from large ice particles (e.g., graupel or hailstones) that produce many raindrops of moderate-to-large and small sizes, which contribute to high Z_{DR}/K_{DP} values. These raindrops can recirculate into updrafts and be lifted to the mixed-phase region, forming the Z_{DR} column first, but then, it collapses as graupel and/or hailstone particles increase. Convection and lightning are enhanced, and a K_{DP} column is formed, which is associated with an increasing number of small-to-moderate hailstones with a significant water fraction. Thus, the Z_{DR} and K_{DP} columns within the reflectivity core are associated with the different stages of an impulse event, the Z_{DR} column indicates the stage in which cold cloud processes are weak, and the K_{DP} column is the opposite of the Z_{DR} column. This may explain the remaining question in Sharma et al. (2021), namely, why the K_{DP} column has a noticeably different pattern than the Z_{DR} column does. Notably, the Z_{DR} column is located at the periphery of the reflectivity core when the Z_{DR} column collapses within the reflectivity core."

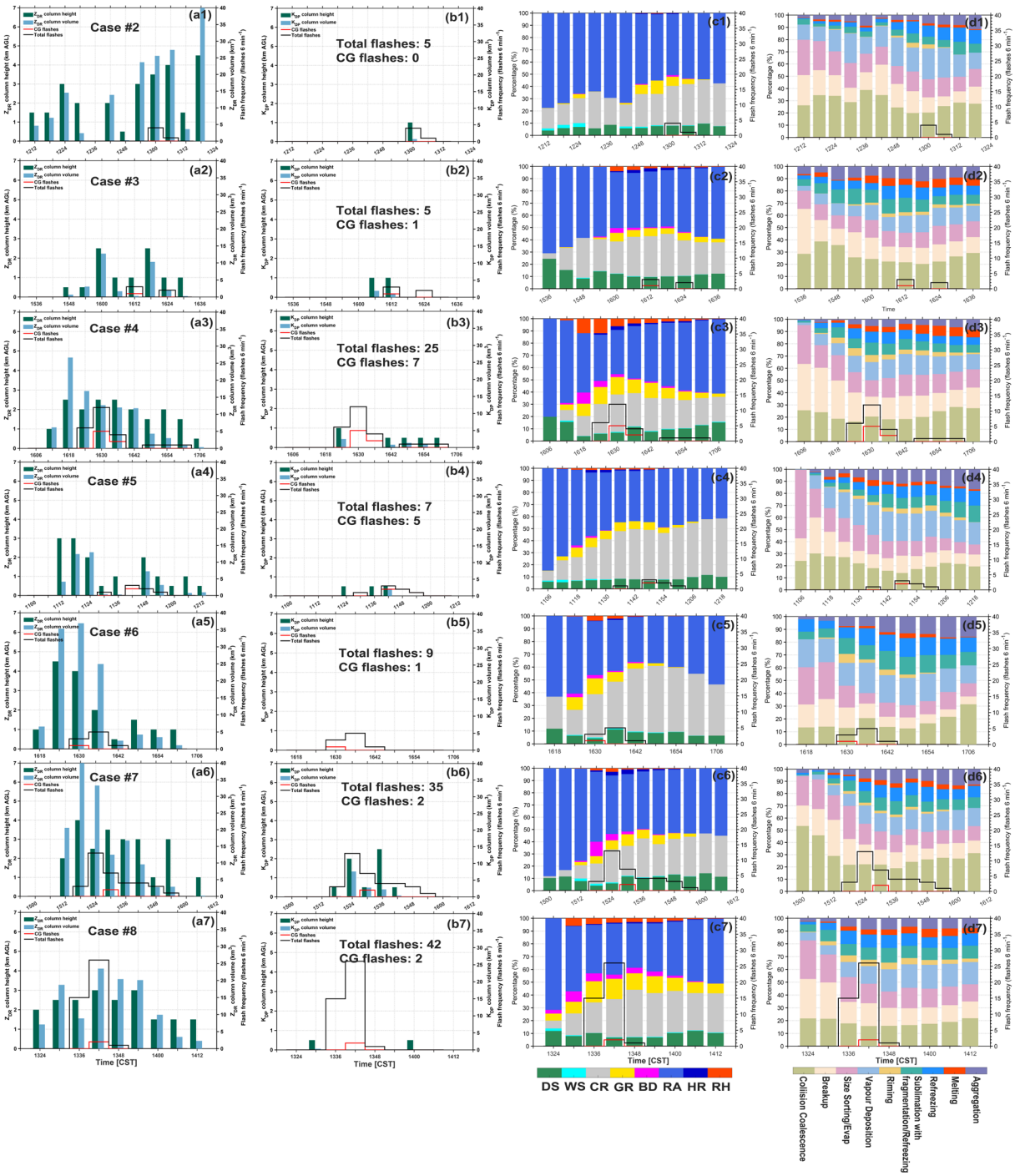

Figure 10. The variation in Z_{DR} column height and volume with the life cycle of thunderstorms (cases #2 to #8) (a1-a7). The variation in the K_{DP} column height and volume with the life cycle of thunderstorms (cases #2 to #8) (b1-b7). The dark green bars indicate the column heights, and the light blue bars indicate the column volumes. The texts display the number of total flashes and CG flashes in a thunderstorm. The variation in percentages of hydrometeor types with the life cycle of thunderstorms (cases #2 to #8) (c1-c7). The variation in percentages of microphysical

fingerprints with the life cycle of thunderstorms (cases #2 to #8) (d1-d7). The black stair lines indicate the total flashes, and the red stair lines indicate the CG flashes.

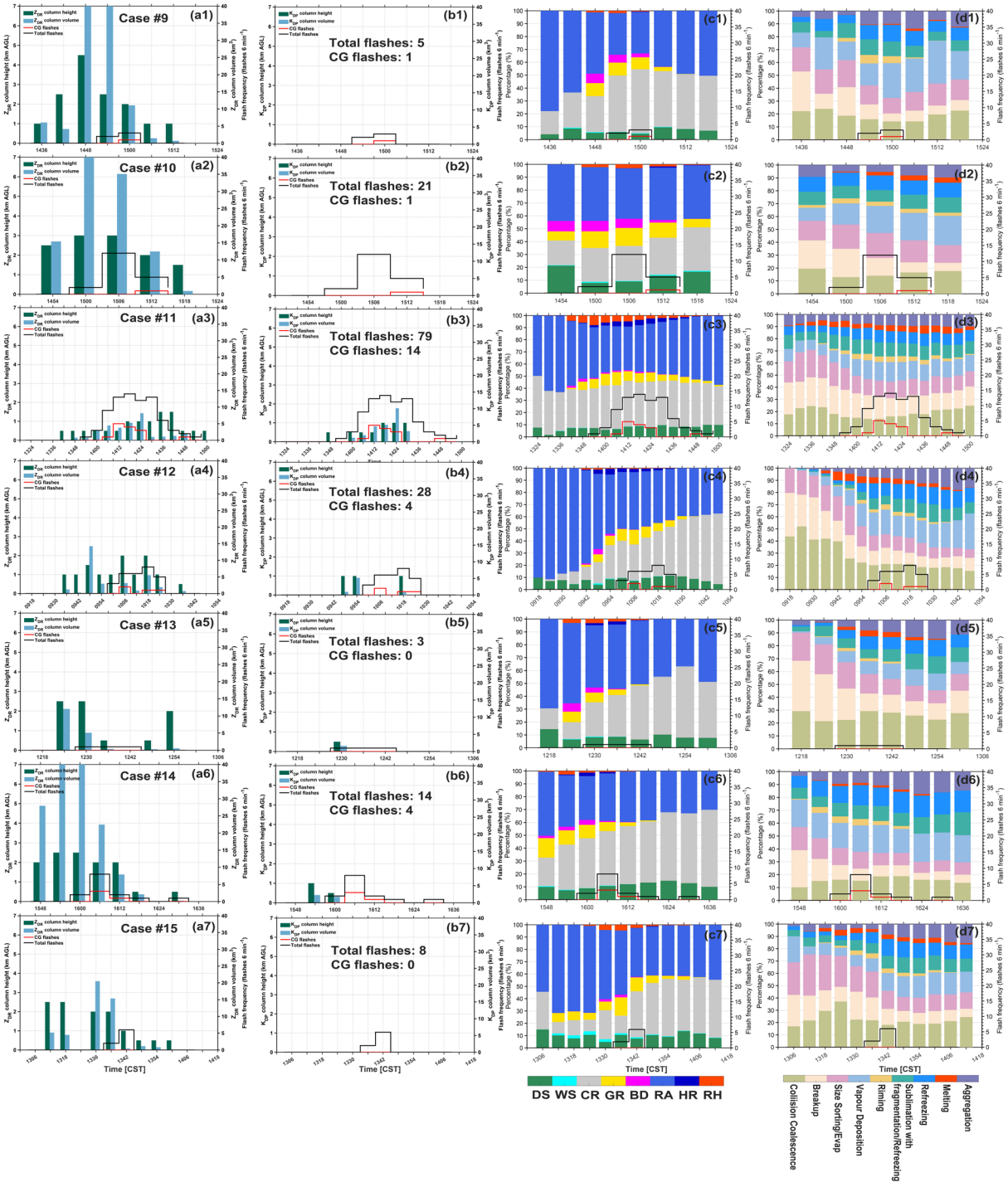

Figure 11. The variation in Z_{DR} column height and volume with the life cycle of thunderstorms (cases #9 to #15) (a1-a7). The variation in the K_{DP} column height and volume with the life cycle of thunderstorms (cases #9 to #15) (b1-b7). The dark green bars indicate the column heights, and the light blue bars indicate the column volumes. The texts display the number of total flashes and CG flashes in a thunderstorm. The variation in percentages of hydrometeor types with the life

cycle of thunderstorms (cases #9 to #15) (c1-c7). The variation in percentages of microphysical fingerprints with the life cycle of thunderstorms (cases #9 to #15) (d1-d7). The black stair lines indicate the total flashes, and the red stair lines indicate the CG flashes.

Bruning, E. C., Brunner, K. N., van Lier-Walqui, M., Logan, T. and Matsui, T.: Lightning and Radar Measures of Mixed-Phase Updraft Variability in Tracked Storms during the TRACER Field Campaign in Houston, Texas. Monthly Weather Review, 152, 2753-2769, https://doi.org/10.1175/MWR-D-24-0060.1, 2024.

Fridlind, A. M., van Lier-Walqui, M., Collis, S., Giangrande, S. E., Jackson, R. C., Li, X., Matsui, T., Orville, R., Picel, M. H., Rosenfeld, D., Ryzhkov, A., Weitz, R., and Zhang, P.: Use of polarimetric radar measurements to constrain simulated convective cell evolution: a pilot study with Lagrangian tracking. Atmospheric Measurement Techniques, 12(6), 2979-3000, https://doi.org/10.5194/amt-12-2979-2019, 2019.

Sharma, M., Tanamachi, R. L. and Bruning, E. C.: Investigating Temporal Characteristics of Polarimetric and Electrical Signatures in Three Severe Storms: Insights from the VORTEX-Southeast Field Campaign. Monthly Weather Review, 152(7): 1511-1536, https://doi.org/10.1175/MWR-D-23-0144.1, 2024.

Sharma, M., Tanamachi, R. L., Bruning, E. C. and Calhoun, K. M.: Polarimetric and Electrical Structure of the 19 May 2013 Edmond–Carney, Oklahoma, Tornadic Supercell. Monthly Weather Review, 149(7): 2049-2078, https://doi.org/10.1175/MWR-D-20-0280.1, 2021.

4. Line 157: Authors claim that their study is sufficient to establish a connection between "four parameters" and lightning using a single isolated storm case. However, despite numerous studies, including Sharma et al., 2024, which have observed a close correlation between these four parameters and lightning activity, they acknowledge the potential influence of other factors on this relationship. For instance, between ZDR or KDP volumes and total lightning flash rates. Therefore, the primary question arises: are these four parameters truly sufficient, and how do the authors substantiate this belief?

Reply: Thank you for this insightful comment. We believe that the key to answering this question is providing a reasonable explanation or physical mechanism to explain these variations in the relationships between Z_{DR} or K_{DP} column volumes and total lightning flash rates (e.g., the observations in Sharma et al., 2024 or Sharma et al., 2021).

To solve this problem, we explore the polarimetric and microphysical structures related to impulse events (impulses in vertical velocity) and lightning activity. The differences

in the formation of Z_{DR} and K_{DP} columns with related microphysics and dynamics are clarified in the draft. The results can answer the remaining question in Sharma et al. (2021), namely, why does the K_{DP} column have a noticeably different pattern than the Z_{DR} column, as does Sharma et al. (2024). Please see in mms (Lines 451−508; 719−748).

In addition, more cases and parameters are included in this study to strengthen our results. The related content has already been presented in your first comment. The methods for newly introduced parameters are described in **Section 2.2**. Please see in mms (Lines 298−330).

Lines 451−508 in mms:

"**3.2 Vertical structures of microphysics related to lightning activity**

To study the vertical thunderstorm structure related to lightning activity, we explore the vertical structures of polarimetric radar variables and microphysics, in combination with 3D lightning location data. Figure 7 displays the cross sections of polarimetric radar variables (Z_H, Z_{DR}, and K_{DP}) and microphysics (hydrometeor types and microphysical fingerprints) from the Cartesian grid of the studied isolated thunderstorm. At 18:00 CST (Figure 7 a1-e1), the lightning activity begins, and the locations of the flash sources are high and correspond mainly to graupel particles. Riming occurrence surrounds the flash sources. The Z_{DR} column and reflectivity core (≥ 40 dBZ) begin to separate, having previously been overlapping during the initial development stage of the thunderstorm (Figure 4a, b). Then, at 18:06 CST (Figure 7 a2-e2), riming begins obviously, the echoes strengthen (≥ 55 dBZ), and the heights of the strong echoes are lifted. This finding indicates that the convective strength or updrafts are obviously increased and that the cold cloud processes are heavily. The lightning activity reached the first peak, where the locations of the flash sources mainly corresponded to graupel and ice particles. Moreover, the Z_{DR} column is located at the periphery of the reflectivity core, and high K_{DP} values occur and correspond to heavy rain particles, which are associated with large ice particles (e.g., hailstones) melting, raindrops coalescence and/or break. This phenomenon is consistent with that the K_{DP} tends to be directly proportional to the rain mixing ratio (Snyder et al., 2017).

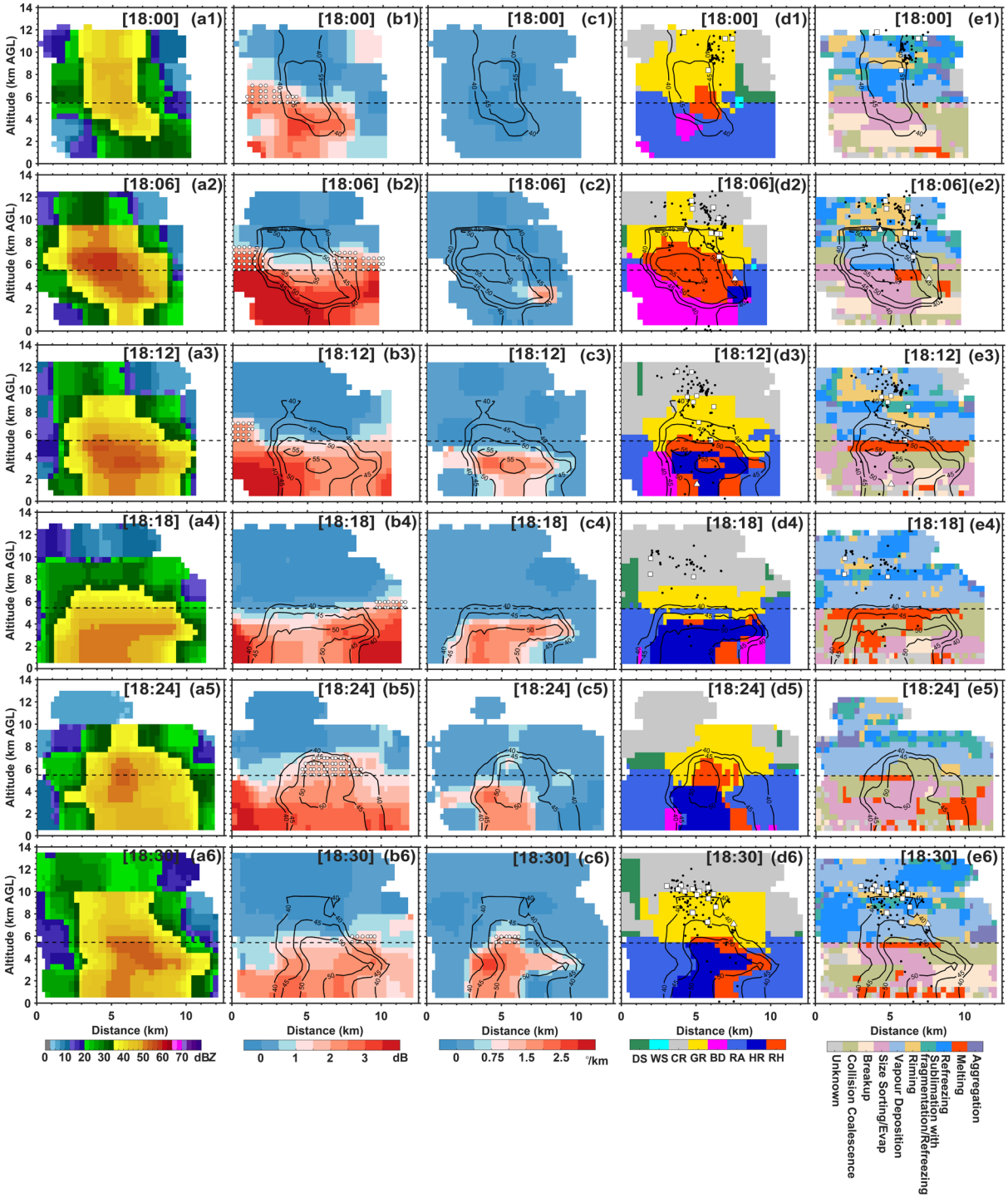

Figure 7. Cross sections of polarimetric radar variables (Z_H, Z_{DR}, and K_{DP}) and microphysics (hydrometeor types and microphysical fingerprints) from the Cartesian grid of the isolated thunderstorm (case #1). At 18:00 CST (a1-e1), 18:06 CST (a2-e2), 18:12 CST (a3-e3), 18:18 CST (a4-e4), 18:24 CST (a5-e5), and 18:30 CST (a6-e6). The black dashed line indicates the 0°C isotherm height. The white dots indicate the areas of the identified Z_{DR}/K_{DP} columns. The black contours with values indicate the reflectivity structure. The black dots indicate the flash

sources, the white square represents the first source of the intracloud flash, and the triangle represents the CG flash.

Subsequently, the lightning activity weakened at 18:12 and 18:18 CST. During this stage (Figure 7 a3-e3, a4-e4), the reflectivity core is landing and large ice particles above the melting level decrease, corresponding to heavy melting and indicating increasing downdrafts. Although Z_{DR} columns are present, they can only indicate updrafts around the reflectivity core. However, the reflectivity core was lifted again at 18:24 CST (Figure 7 a5). The contents of rain and hail mixtures and graupel clearly increased (Figure 7 d5). This indicates that the convective strength or updrafts are increased. Notably, the Z_{DR} column and reflectivity core overlap again, just as occurred during the initial development of the thunderstorm (Figure 4a, b; Figure 7 b5). Although a few high K_{DP} values occurred above the melting level, a K_{DP} column formed during the next 6 minutes (Figure 7 c5, c6). At 18:30 CST (Figure 7 a6-e6), the lightning activity reaches the second peak, and the riming process surrounds these flash sources. The Z_{DR} column within the reflectivity core quickly collapses with the occurrence of abundant graupel particles.

In total, this thunderstorm shows two impulses in vertical velocity, which correspond to two lightning activity peaks. When the first impulse event initially develops, the Z_{DR} column is obvious and overlaps with the reflectivity core; however, the region of the Z_{DR} column within the reflectivity core will collapse, with abundant graupel particles forming by riming or freezing, stimulating updrafts and intensified lightning. When large ice particles (e.g., graupel or hailstone) subsequently decrease, indicating the end of the first impulse event, melting and shedding processes occur, resulting in more raindrops (many moderate-to-large and small raindrops) contributing to high Z_{DR}/K_{DP} values. These raindrops could recirculate into the updrafts and be lifted to the mixed-phase region, forming the Z_{DR} column first, and raindrops could transfer to abundant graupel and even hailstones, releasing latent heat and thus invigorating updrafts again (indicating the second impulse event). However, the Z_{DR} column within the reflectivity core will collapse with increasing amounts of graupel and/or hailstone particles, but the K_{DP} column will occur; this can be explained by the increased K_{DP} values at the column top being associated with an increasing number of small-to-moderate hailstones with significant water fractions (Snyder et al., 2017). The lightning activity also reaches a peak value.

Thus, the Z_{DR} column within the reflectivity core is likely an indicator of imminent convection invigoration via latent heat release and then the formation of abundant graupel particles promotes lightning activity via noninductive charging; the K_{DR} column

is highly related to cold cloud processes, replacing Z_{DR} column to indicate updrafts within the reflectivity core when obvious graupels and hailstones occur."

Lines 719−748 in mms:

"As discussed in Section 3.2, lightning activity is indeed related to dynamic variation and impulses in vertical velocity, which is consistent with the findings of previous studies (e.g., Bruning et al., 2024; Sharma et al., 2024; Sharma et al., 2021). The unsteady Z_{DR} and K_{DP} columns are tied to unsteady updrafts associated with thermal bubbles, which are relatively short-lived and thus indicate an impulse in vertical velocity. In this way, the variations in the Z_{DR} and K_{DP} columns can indicate lightning activity. Although this hypothesis is reasonable and supported by observations through the microphysical signatures of large-drop lofting and glaciation corresponding to the Z_{DR} and K_{DP} columns (Bruning et al., 2024; Fridlind et al., 2019); however, the observations of Sharma et al. (2024) and Sharma et al. (2021) revealed that the K_{DP} column volumes (or mean K_{DP} values within a segmented K_{DP} column) have noticeably different pattern than the Z_{DR} column volumes (or mean Z_{DR} values within a segmented Z_{DR} column), which has remained a question in Sharma et al. (2021).

In this study, we explore the polarimetric and microphysical structures related to impulse events and lightning activity. The results indicate that the column within the reflectivity core is only the Z_{DR} column in which the impulse event initially develops; then, the supercooled raindrops indicated by the Z_{DR} column transfer to abundant graupel and/or hailstone particles, releasing latent heat and thus invigorating convection; accompanying the Z_{DR} column within the reflectivity core, it collapses, and lightning intensifies. Moreover, the formation of the K_{DP} column requires melting and shedding processes from large ice particles (e.g., graupel or hailstones) that produce many raindrops of moderate-to-large and small sizes, which contribute to high Z_{DR}/K_{DP} values. These raindrops can recirculate into updrafts and be lifted to the mixed-phase region, forming the Z_{DR} column first, but then, it collapses as graupel and/or hailstone particles increase. Convection and lightning are enhanced, and a K_{DP} column is formed, which is associated with an increasing number of small-to-moderate hailstones with a significant water fraction. Thus, the Z_{DR} and K_{DP} columns within the reflectivity core are associated with the different stages of an impulse event, the Z_{DR} column indicates the stage in which cold cloud processes are weak, and the K_{DP} column is the opposite of the Z_{DR} column. This may explain the remaining question in Sharma et al. (2021), namely, why the K_{DP} column has a noticeably different pattern than the Z_{DR} column does. Notably, the Z_{DR} column is located at the periphery of the reflectivity core when the Z_{DR} column collapses within the reflectivity core."

Lines 298−330 in mms:

"To further explore the characteristics of the microphysics related to the Z_{DR}/K_{DP} column and lightning within these thunderstorms, hydrometeor identification method involving the fuzzy-logic algorithm (as in Zhao et al., 2021b) and the microphysical fingerprint (following Kumjian et al., 2022) are conducted. Identifying polarimetric radar "fingerprints" of ongoing microphysical processes was introduced by Kumjian (2012); these fingerprints are defined as vertical changes in two (e.g., Z_H, Z_{DR}) or more of the dual-polarization radar variables (Kumjian et al., 2022).

As suggested by Kumjian et al. (2022), the co-polar correlation coefficient (CC) is neglected in most of the fingerprints discussed but it is important to indicate the melting process; thus, we added the changes in the CC towards the ground to identify the melting process. The changes in the polarimetric radar variables towards the ground for riming and aggregation are the same (Kumjian et al., 2022); however, the riming process is valuable for studying lightning activity. Thus, we followed the method for identifying the aggregation and graupel particles in Park et al. (2009), namely, we utilized the discriminated convective and stratiform echoes to determine where riming or aggregation processes occur. If the echo is classified as convective, then the aggregation process is not allowed within a whole vertical column; conversely, the riming process is excluded in the stratiform case.

In addition, the 0°C isotherm height is used to discriminate warm-rain processes and mixed-phase processes; notably, this rule introduces potential errors when it is used where the Z_{DR}/K_{DP} column is used. Specifically, the polarimetric characteristics of collision-coalescence and size sorting (or evaporation) processes above the 0°C isotherm height are regarded as vapour deposition and refreezing processes, respectively. In this study, we utilize the identified and quantified Z_{DR}/K_{DP} columns to correct this possible error. A summary of the changes in the polarimetric radar variables towards the ground and additional conditions for different microphysical processes is displayed in Table 2. To characterize the microphysical fingerprints in this study, the changes in the polarimetric radar variables towards the ground are computed between two adjacent grids in the vertical direction (for example, $\Delta Z_H\,(x, y, z_1) = Z_H\,(x, y, z_2) - Z_H\,(x, y, z_1)$, x, y, and z are the three dimensions in the Cartesian coordinate system; z_1 is 500 m in height, and z_2 is 1000 m in height). The minimum thresholds of $\Delta Z_H > 0.002$ dB/km and $\Delta Z_{DR} > 0.0001$ dB/km are applied to avoid false classifications based on noise present in the data, as in Kumjian et al. (2022).

Table 2. Changes in the polarimetric radar variables towards the ground for different microphysical processes. An increase in that radar variable between the top and bottom of the profile is indicated by a positive sign +, whereas a decrease is indicated by a negative sign.

Microphysical processes	ΔZ_H	ΔZ_{DR}	ΔCC	Convective/Stratiform area	Z_{DR}/K_{DP} column
Collision-Coalescence	+	+	/	/	√
Breakup	−	−	/	/	/
Size Sorting/Evaporation	−	+	/	/	√
Vapour Deposition	+	+	/	/	×
Aggregation	+	−	/	Stratiform area	/
Riming	+	−	/	Convective area	/
Sublimation (with fragmentation)/Refreezing	−	−	/	/	/
Refreezing	−	+	/	/	×
Melting	+	+	−	/	/

"

Kumjian, M. R.: The Impact of Precipitation Physical Processes on the Polarimetric Radar Variables. Ph. D. Dissertation, The University of Oklahoma, Norman, OK, USA, 327p., 2012.

Kumjian, M. R., Prat, O. P., Reimel, K. J., van Lier-Walqui, M. and Morrison, H. C.: Dual-Polarization Radar Fingerprints of Precipitation Physics: A Review. Remote Sensing, 14, 3706, https://doi.org/10.3390/rs14153706, 2022.

Park, H. S., Ryzhkov, A. V., Zrnić, D. S., and Kim, K.: The Hydrometeor Classification Algorithm for the Polarimetric WSR-88D: Description and Application to an MCS. Weather and Forecasting, 24: 730-748, https://doi.org/10.1175/2008WAF2222205.1, 2009.

Ryzhkov, A., and Zrnić, D.: Assessment of Rainfall Measurement That Uses Specific Differential Phase. Journal of Applied Meteorology and Climatology, 35: 2080-2090, https://doi.org/10.1175/1520-0450(1996)035<2080:AORMTU>2.0.CO;2, 1996.

Zhao, C., Zheng, D., Zhang, Y. J., Liu, X., Zhang, Y., Yao, W., and Zhang, W.: Characteristics of cloud microphysics at positions with flash initiations and channels in convection and stratiform areas of two squall lines, Journal of Tropical Meteorology, 37: 358-369, doi:10.16032/j.issn.1004-4965.2021.035, 2021b.

5. Line 192: Briefly describe "the same method" here.

Reply: The draft has been revised as suggested. Please see in mms (Lines 233−236).

Lines 233−236 in mms:

"A potential discharge pulse event of one lightning flash should occur within 0.4 s of the previous discharge pulse event and within 0.6 s and 4 km of any other discharge pulse event of this lightning flash."

6. Section 2.2: What equations did the authors use to retrieve the cloud microphysical parameters? How large are the uncertainties of these retrieval methods? Are the retrieval methods suitable for the current radar used in this study? How did the authors classify the particle categories, especially the ice particles in the mixed-phase regions?

Reply: Thank you very much for your careful reading and comments, which have helped us improve the readability of this manuscript. The details about this method, including the equations and uncertainties, have been added to the revised draft as suggested. The retrieval methods are suitable for the current radar used in this study on the basis of local observations and empirical relationships. Moreover, we discuss the applicability of the method for investigation in this study. Please see in mms (Lines 247−284).

Pruppacher and Klett (1997) assumed that precipitation-sized ice particles were more spherically symmetrical or tumble. The low dielectric constant and significant canting behaviour of ice particles likely result in a near-zero Z_{DR} (e.g., Seliga and Bringi, 1976). Therefore, the horizontal reflectivity and vertical reflectivity are equal for ice particles, as "effective spheres", and the Z_{DP} is influenced solely by raindrops. Thus, rain and ice water contents are discriminated according to the Z_{DP} method. Then, the estimated ice masses are assigned to graupel masses on the basis of scattering properties, namely, where the Z_H values exceed 35 dBZ (Carey and Rutledge, 2000; Kumjian, 2013a, b; Zhao, et al., 2021b).

In addition, to further explore the characteristics of the microphysics related to the Z_{DR}/K_{DP} column and lightning within these thunderstorms, hydrometeor identification methods involving the fuzzy-logic algorithm (as in Zhao et al., 2021b) and the microphysical fingerprints (following Kumjian et al., 2022) are conducted. Identifying polarimetric radar "fingerprints" of ongoing microphysical processes was introduced by Kumjian (2012); these fingerprints are defined as vertical changes in two (e.g., Z_H, Z_{DR}) or more of the dual-polarization radar variables (Kumjian et al., 2022). For more details, please see in mms (Lines 298−330).

Lines 247−284 in mms:

"To estimate the precipitation-sized ice mass (e.g., graupel, hail, and frozen drops) and the content of supercooled raindrops within the mixed-phase zone, an approach on the basis of difference reflectivity (Z_{DP}, dB) is applied (Carey and Rutledge, 2000; Straka et al., 2000).

$$Z_h = (4\lambda^4/\pi^4|K_w|^2)\langle|S_{hh}|^2\rangle \quad (1)$$

$$Z_v = (4\lambda^4/\pi^4|K_w|^2)\langle|S_{vv}|^2\rangle \quad (2)$$

$$Z_{DP} = 10\log_{10}(Z_h - Z_v), \text{ for } Z_h > Z_v \quad (3)$$

S_{ij} refers to an element of the backscattering matrix of a hydrometeor (Zrnić, 1991). The first subscript *i* indicates the polarization of the backscattered field (*h* is horizontal, *v* is vertical), and the second subscript *j* indicates the polarization of the incident field. $K_w=(\epsilon_w-1)/(\epsilon_w+2)$ is the factor associated with the dielectric constant of water, and ϵ_w is the dielectric constant. λ is the radar wavelength. The brackets indicate expectations expressed in terms of the distribution of mean hydrometeor properties such as shape, size, fall orientation, particle density, canting angle, dielectric constant, and others.

Pruppacher and Klett (1997) assumed that precipitation-sized ice particles were more spherically symmetrical or tumble. The low dielectric constant and significant canting behaviour of ice particles likely result in a near-zero Z_{DR} (e.g., Seliga and Bringi, 1976). Therefore, the horizontal reflectivity and vertical reflectivity are equal for ice particles, as "effective spheres", and Z_{DP} is solely influenced by raindrops. If the relationship between horizontal reflectivity and Z_{DP} (raindrops) is known, the horizontal reflectivity of raindrops can be derived. The relationship between the horizontal reflectivity of raindrops and Z_{DP} (raindrops) is derived from 2-year disdrometer data in Guangdong Province (Li et al., 2019), which is suitable for the current radar used in this study:

$$Z_H^{rain}=0.0044Z_{DP}^2+0.58054Z_{DP}+16.591 \quad (4)$$

Then, the ice echo intensity Z_H^{ice} can be expressed as $Z_H - Z_H^{rain}$. The standard error for the relationship between horizontal reflectivity and Z_{DP} is consistently approximately 1 dB (Carey and Rutledge, 2000). If $Z_H - Z_H^{rain} < 1$ dB, which is below the melting layer, $Z_h^{ice} = 0$ mm^{6}m^{-3}, $Z_H^{rain}=10\log_{10}(Z_h^{rain})$, and $Z_h^{rain} = Z_h$. In contrast, above the melting layer, if $Z_H - Z_H^{ice} < 1$ dB, then $Z_h^{rain} = 0$ mm^{6}m^{-3}, and $Z_h^{ice} = Z_h$ (Carey and Rutledge, 2000). The estimates of rain mass (M_w, g m^{-3}) and ice mass (M_{ice}, g m^{-3}) are derived via the following reflectivity–mass relationships (Chang et al., 2015; Zhao et al., 2022):

$$M_w = 3.44\times10^{-3}\left(Z_h^{rain}\right)^{4/7} \quad (5)$$

$$M_i = 1000\pi\rho_i N_0^{3/7}\left(\frac{5.28\times10^{-18}Z_h^{ice}}{720}\right)^{4/7} \quad (6)$$

where ρ_i indicates the ice density (kg m^{-3}), $N_0=4\times10^6$ m^{-4}. The estimated ice mass from the horizontal reflectivity of ice particles is proportional to the actual ice mass and depends on the variability in the intercept parameter of an assumed inverse exponential distribution for ice and the ice density; thus, the trends of the estimated ice mass are deemed sufficient to investigate lightning activity. Importantly, the Z_{DP} can

differentiate between ice and rain only if the Z_H is sufficiently large (i.e., diameter ≥ 1 mm); under such conditions, the raindrop is characterized by significant oblateness (Carey and Rutledge, 2000; Green, 1975)."

Lines 298−330 in mms:

"To further explore the characteristics of the microphysics related to the Z_{DR}/K_{DP} column and lightning within these thunderstorms, hydrometeor identification method involving the fuzzy-logic algorithm (as in Zhao et al., 2021b) and the microphysical fingerprint (following Kumjian et al., 2022) are conducted. Identifying polarimetric radar "fingerprints" of ongoing microphysical processes was introduced by Kumjian (2012); these fingerprints are defined as vertical changes in two (e.g., Z_H, Z_{DR}) or more of the dual-polarization radar variables (Kumjian et al., 2022).

As suggested by Kumjian et al. (2022), the co-polar correlation coefficient (CC) is neglected in most of the fingerprints discussed but it is important to indicate the melting process; thus, we added the changes in the CC towards the ground to identify the melting process. The changes in the polarimetric radar variables towards the ground for riming and aggregation are the same (Kumjian et al., 2022); however, the riming process is valuable for studying lightning activity. Thus, we followed the method for identifying the aggregation and graupel particles in Park et al. (2009), namely, we utilized the discriminated convective and stratiform echoes to determine where riming or aggregation processes occur. If the echo is classified as convective, then the aggregation process is not allowed within a whole vertical column; conversely, the riming process is excluded in the stratiform case.

In addition, the 0°C isotherm height is used to discriminate warm-rain processes and mixed-phase processes; notably, this rule introduces potential errors when it is used where the Z_{DR}/K_{DP} column is used. Specifically, the polarimetric characteristics of collision-coalescence and size sorting (or evaporation) processes above the 0°C isotherm height are regarded as vapour deposition and refreezing processes, respectively. In this study, we utilize the identified and quantified Z_{DR}/K_{DP} columns to correct this possible error. A summary of the changes in the polarimetric radar variables towards the ground and additional conditions for different microphysical processes is displayed in Table 2. To characterize the microphysical fingerprints in this study, the changes in the polarimetric radar variables towards the ground are computed between two adjacent grids in the vertical direction (for example, $\Delta Z_H(x, y, z_1) = Z_H(x, y, z_2) - Z_H(x, y, z_1)$, x, y, and z are the three dimensions in the Cartesian coordinate system; z_1 is 500 m in height, and z_2 is 1000 m in height). The minimum thresholds of ΔZ_H >

0.002 dB/km and ΔZ_{DR} > 0.0001 dB/km are applied to avoid false classifications based on noise present in the data, as in Kumjian et al. (2022).

Table 2. Changes in the polarimetric radar variables towards the ground for different microphysical processes. An increase in that radar variable between the top and bottom of the profile is indicated by a positive sign +, whereas a decrease is indicated by a negative sign.

Microphysical processes	ΔZ_H	ΔZ_{DR}	ΔCC	Convective/Stratiform area	Z_{DR}/K_{DP} column
Collision-Coalescence	+	+	/	/	√
Breakup	−	−	/	/	/
Size Sorting/Evaporation	−	+	/	/	√
Vapour Deposition	+	+	/	/	×
Aggregation	+	−	/	Stratiform area	/
Riming	+	−	/	Convective area	/
Sublimation (with fragmentation)/Refreezing	−	−	/	/	/
Refreezing	−	+	/	/	×
Melting	+	+	−	/	/

”

Carey, L. D. and Rutledge, S. A.: The Relationship between Precipitation and Lightning in Tropical Island Convection: A C-Band Polarimetric Radar Study. Monthly Weather Review, 128(8): 2687-2710, 10.1175/1520-0493(2000)128<2687:TRBPAL>2.0.CO;2, 2000.

Chang, W., Lee, W. and Liou, Y.: The kinematic and microphysical characteristics and associated precipitation efficiency of subtropical convection during SoWMEX/TiMREX. Monthly Weather Review, 143(1): 317–340. https://doi.org/10.1175/MWR-D-14-00081.1, 2015.

Green, A. W.: An Approximation for the Shapes of Large Raindrops. Journal of Applied Meteorology and Climatology, 14: 1578-1583, https://doi.org/10.1175/1520-0450(1975)014<1578:AAFTSO>2.0.CO;2, 1975.

Li, H. Q., Wan, Q., Peng, D., Liu, X. and Xiao, H.: Multiscale analysis of a record-breaking heavy rainfall event in Guangdong, China. Atmospheric Research, 232: 104703. https://doi.org/10.1016/j.atmosres.2019.104703, 2019.

Straka, J. M., Zrnić, D. S. and Ryzhkov, A. V.: Bulk Hydrometeor Classification and Quantification Using Polarimetric Radar Data: Synthesis of Relations. Journal of Applied Meteorology and Climatology, 39: 1341-1372, https://doi.org/10.1175/1520-0450(2000)039<1341:BHCAQU>2.0.CO;2, 2000.

Zhao, C., Zhang, Y., Zheng, D., Liu, X., Zhang, Y., Fan, X., Yao, W. and Zhang, W.: Using Polarimetric Radar Observations to Characterize First Echoes of Thunderstorms and Nonthunderstorms: A Comparative Study. Journal of Geophysical Research: Atmospheres, 127(23): e2022JD036671, https://doi.org/10.1029/2022JD036671, 2022.

Zrnić, D. S.: Complete Polarimetric and Doppler Measurements with a Single Receiver Radar. Journal of Atmospheric and Oceanic Technology, 8: 159-165, https://doi.org/10.1175/1520-0426(1991)008<0159:CPADMW>2.0.CO;2, 1991.

7. Line 205: What definition of "difference reflectivity" here? How is it different from ZDR? Why are the units of ZDP in dB?

Reply: We have added the definition and equation of "difference reflectivity (Z_{DP})" to the draft as suggested. Please see in mms (Line 252).

$Z_{DP} = 10\log_{10}(Z_h - Z_v)$, for $Z_h > Z_v$……(R1)

$Z_{DR} = 10\log_{10}\left(\frac{Z_h}{Z_v}\right)$, ……(R2)

Z_h or Z_v is the horizontal reflectivity factor or vertical reflectivity factor, in mm^6m^{-3}. Eq. R1 is for Z_{DP}, and Eq. R2 is for Z_{DR}.

8. Line 216: Please justify using the assumption of "inverse exponential distribution".

Reply: The equations of the retrieval method have been added as suggested to decrease confusion. Please see in mms (Lines 276−278).

Lines 276−278 in mms:

"

$$M_w = 3.44 \times 10^{-3}\left(Z_h^{rain}\right)^{4/7} \quad (5)$$

$$M_i = 1000\pi\rho_i N_0^{3/7}\left(\frac{5.28\times10^{-18}Z_h^{ice}}{720}\right)^{4/7} \quad (6)$$

where ρ_i indicates the ice density (kg m^{-3}), N_0=4×10^6 m^{-4}.

9. Line 219: Please justify using the threshold of 35 dBZ for ZH here.

Reply: When the Z_H values exceed 35 dBZ, the reflectivity factor is dominated by graupel particles according to scattering properties; thus, this threshold is usually applied to identify graupel in the hydrometeor identification method (e.g., Park et al., 2009). Therefore, in accordance with previous study (e.g., Carey and Rutledge, 2000), the estimated ice masses were assigned to graupel masses where the Z_H values exceeded 35 dBZ.

We have revised this sentence to decrease confusion. Please see in mms (Lines 285−288).

Lines 285−288 in mms:

"The estimated ice masses are assigned to graupel masses on the basis of scattering properties, namely, where the Z_H values exceed 35 dBZ (Carey and Rutledge, 2000; Kumjian, 2013a, b; Zhao, et al., 2021b). The threshold value is usually applied to identify graupel in hydrometeor identification method (Park et al., 2009)."

10. Line 223-225: Did the authors use the threshold of "2 mm" for D0 to identify ZDR columns? If so, please justify why using 2 mm. Do the results change if changing this threshold?

Reply: There may be some confusion here. We did not use the threshold of "2 mm" for D0 to identify the Z_{DR} column. However, the selection of a 1.5 dB threshold value for the Z_{DR} to identify the Z_{DR} column considers the result of the retrieved D0. The Z_{DR} column above the melting level indicates the presence of a low concentration of large raindrops (>2 mm) (Kumjian et al., 2014).

We have revised the related content to decrease confusion. Please see in mms (Lines 292−296).

Lines 292−296 in mms:

"Z_{DR} columns are associated with low concentration of large raindrops (>2 mm); thus, the median volume diameter D_0 of raindrops is retrieved via the method described by Hu and Ryzhkov (2022) to provide supporting evidence for identifying Z_{DR} columns. Notably, D_0 is not used to identify Z_{DR} columns directly but rather to ensure the threshold value of Z_{DR}, which is utilized to identify Z_{DR} columns directly."

11. Line 260-263: Are there any other situations associated with KDP columns? Why did the authors ask a question here but did not answer it?

Reply: To our knowledge, high K_{DP} values are associated with high number concentration of raindrops or high water fraction in large ice particles, but high K_{DP} values do not mean a K_{DP} column. Observational studies (Hubbert et al., 1998; Loney et al., 2002) have indicated that K_{DP} columns are associated with cold cloud processes and correspond to a wet growth regime.

To address this confusion, we have deleted this question. A discussion of this question can be found in **Section 4**.

12. Lines 332-334: Any evidence supporting this hypothesis?

Reply: We have carefully discussed this hypothesis in **Section 3.2** in the revised draft by exploring the vertical structures of polarimetric radar variables and microphysics in combination with 3D lightning location data.

In total, this thunderstorm shows two impulses in vertical velocity, which correspond to two lightning activity peaks. When the first impulse event initially develops, the Z_{DR} column is obvious and overlaps with the reflectivity core; however, the region of the Z_{DR} column within the reflectivity core will collapse, with abundant graupel particles forming by riming or freezing, stimulating updrafts and intensified lightning. When large ice particles (e.g., graupel or hailstone) subsequently decrease, indicating the end of the first impulse event, melting and shedding processes occur, resulting in more raindrops (many moderate-to-large and small raindrops) contributing to high Z_{DR}/K_{DP} values. These raindrops could recirculate into the updrafts and be lifted to the mixed-phase region, forming the Z_{DR} column first, and raindrops could transfer to abundant graupel and even hailstones, releasing latent heat and thus invigorating updrafts again (indicating the second impulse event). However, the Z_{DR} column within the reflectivity core will collapse with increasing amounts of graupel and/or hailstone particles, but the K_{DP} column will occur; this can be explained by the increased K_{DP} values at the column top being associated with an increasing number of small-to-moderate hailstones with significant water fraction (Snyder et al., 2017). The lightning activity also reaches a peak value.

Thus, the Z_{DR} column within the reflectivity core is likely an indicator of imminent convection invigoration via latent heat release and then the formation of abundant graupel particles promotes lightning activity via noninductive charging; the K_{DR} column is highly related to cold cloud processes, replacing Z_{DR} column to indicate updrafts within the reflectivity core when obvious graupels and hailstones occur.

Please see in mms (Lines 451−508).

Lines 451−508 in mms:

"**3.2 Vertical structures of microphysics related to lightning activity**

To study the vertical thunderstorm structure related to lightning activity, we explore the vertical structures of polarimetric radar variables and microphysics, in combination with 3D lightning location data. Figure 7 displays the cross sections of polarimetric radar variables (Z_H, Z_{DR}, and K_{DP}) and microphysics (hydrometeor types and

microphysical fingerprints) from the Cartesian grid of the studied isolated thunderstorm. At 18:00 CST (Figure 7 a1-e1), the lightning activity begins, and the locations of the flash sources are high and correspond mainly to graupel particles. Riming occurrence surrounds the flash sources. The Z_{DR} column and reflectivity core (≥ 40 dBZ) begin to separate, having previously been overlapping during the initial development stage of the thunderstorm (Figure 4a, b). Then, at 18:06 CST (Figure 7 a2-e2), riming begins obviously, the echoes strengthen (≥ 55 dBZ), and the heights of the strong echoes are lifted. This finding indicates that the convective strength or updrafts are obviously increased and that the cold cloud processes are heavily. The lightning activity reached the first peak, where the locations of the flash sources mainly corresponded to graupel and ice particles. Moreover, the Z_{DR} column is located at the periphery of the reflectivity core, and high K_{DP} values occur and correspond to heavy rain particles, which are associated with large ice particles (e.g., hailstones) melting, raindrops coalescence and/or break. This phenomenon is consistent with that the K_{DP} tends to be directly proportional to the rain mixing ratio (Snyder et al., 2017).

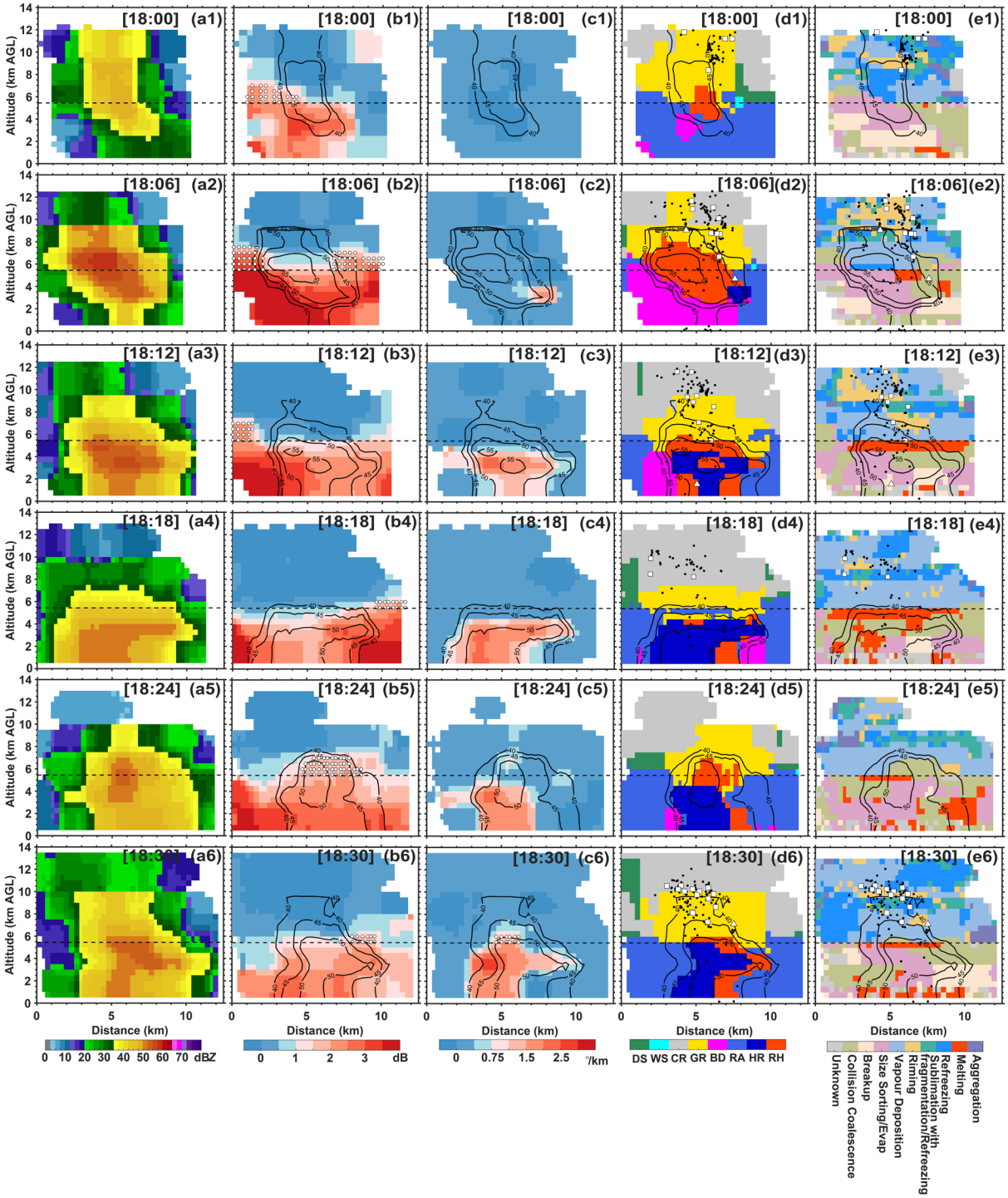

Figure 7. Cross sections of polarimetric radar variables (Z_H, Z_{DR}, and K_{DP}) and microphysics (hydrometeor types and microphysical fingerprints) from the Cartesian grid of the isolated thunderstorm (case #1). At 18:00 CST (a1-e1), 18:06 CST (a2-e2), 18:12 CST (a3-e3), 18:18 CST (a4-e4), 18:24 CST (a5-e5), and 18:30 CST (a6-e6). The black dashed line indicates the 0°C isotherm height. The white dots indicate the areas of the identified Z_{DR}/K_{DP} columns. The black contours with values indicate the reflectivity structure. The black dots indicate the flash

sources, the white square represents the first source of the intracloud flash, and the triangle represents the CG flash.

Subsequently, the lightning activity weakened at 18:12 and 18:18 CST. During this stage (Figure 7 a3-e3, a4-e4), the reflectivity core is landing and large ice particles above the melting level decrease, corresponding to heavy melting and indicating increasing downdrafts. Although Z_{DR} columns are present, they can only indicate updrafts around the reflectivity core. However, the reflectivity core was lifted again at 18:24 CST (Figure 7 a5). The contents of rain and hail mixtures and graupel clearly increased (Figure 7 d5). This indicates that the convective strength or updrafts are increased. Notably, the Z_{DR} column and reflectivity core overlap again, just as occurred during the initial development of the thunderstorm (Figure 4a, b; Figure 7 b5). Although a few high K_{DP} values occurred above the melting level, a K_{DP} column formed during the next 6 minutes (Figure 7 c5, c6). At 18:30 CST (Figure 7 a6-e6), the lightning activity reaches the second peak, and the riming process surrounds these flash sources. The Z_{DR} column within the reflectivity core quickly collapses with the occurrence of abundant graupel particles.

In total, this thunderstorm shows two impulses in vertical velocity, which correspond to two lightning activity peaks. When the first impulse event initially develops, the Z_{DR} column is obvious and overlaps with the reflectivity core; however, the region of the Z_{DR} column within the reflectivity core will collapse, with abundant graupel particles forming by riming or freezing, stimulating updrafts and intensified lightning. When large ice particles (e.g., graupel or hailstone) subsequently decrease, indicating the end of the first impulse event, melting and shedding processes occur, resulting in more raindrops (many moderate-to-large and small raindrops) contributing to high Z_{DR}/K_{DP} values. These raindrops could recirculate into the updrafts and be lifted to the mixed-phase region, forming the Z_{DR} column first, and raindrops could transfer to abundant graupel and even hailstones, releasing latent heat and thus invigorating updrafts again (indicating the second impulse event). However, the Z_{DR} column within the reflectivity core will collapse with increasing amounts of graupel and/or hailstone particles, but the K_{DP} column will occur; this can be explained by the increased K_{DP} values at the column top being associated with an increasing number of small-to-moderate hailstones with significant water fraction (Snyder et al., 2017). The lightning activity also reaches a peak value.

Thus, the Z_{DR} column within the reflectivity core is likely an indicator of imminent convection invigoration via latent heat release and then the formation of abundant graupel particles promotes lightning activity via noninductive charging; the K_{DR} column

is highly related to cold cloud processes, replacing Z_{DR} column to indicate updrafts within the reflectivity core when obvious graupels and hailstones occur."

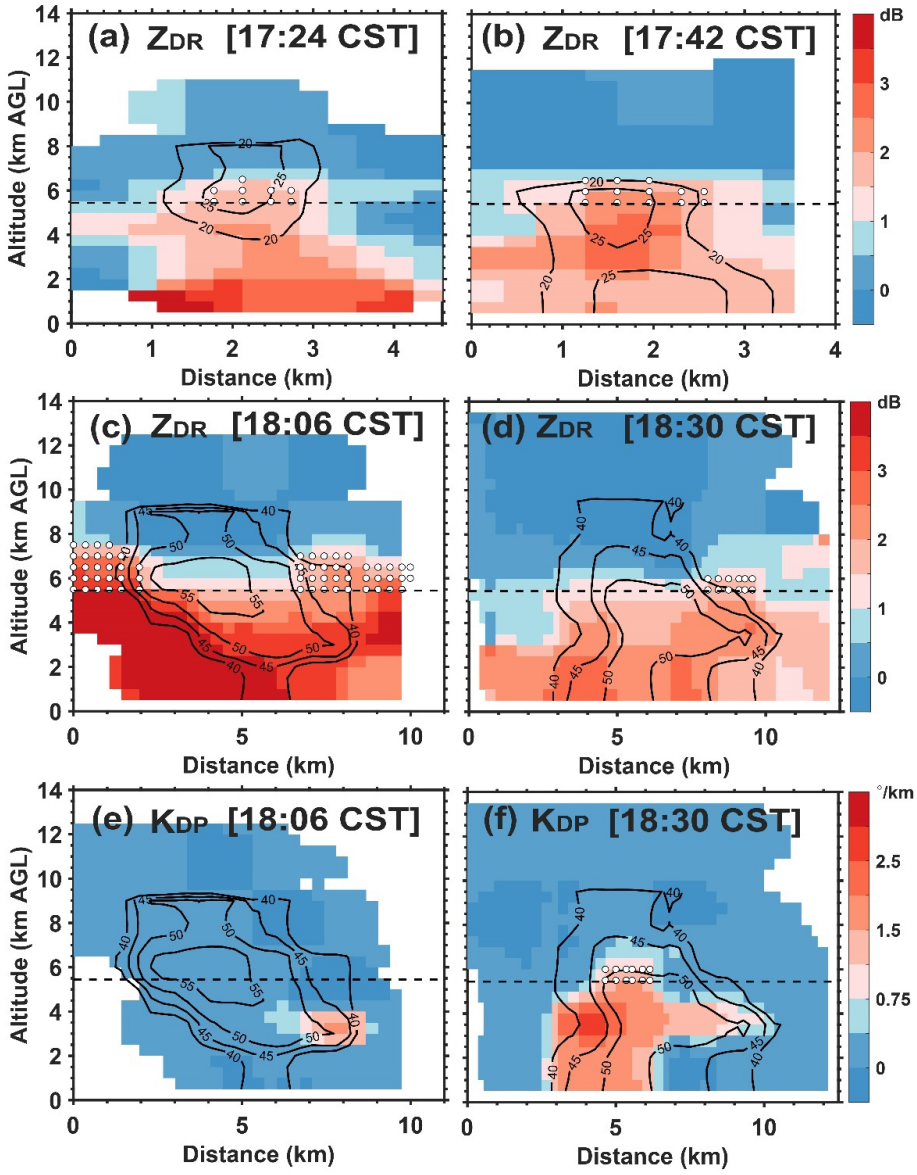

Figure 4. Cross sections from the Cartesian grid of the studied isolated thunderstorm at (a) 17:24 CST, Z_{DR}; (b) 17:42 CST, Z_{DR}; (c) 18:06 CST, Z_{DR}; (d) 18:30 CST, Z_{DR}; (e) 18:06 CST, K_{DP}; and (f) 18:30 CST, K_{DP}. The black dashed line indicates the 0°C isotherm height. The white dots indicate the areas of the identified Z_{DR}/K_{DP} columns. The black contours with values indicate the reflectivity structure. AGL (above ground level).

13. Lines 354-357: Quantify the relationship.

Reply: The description of this sentence is unreasonable, as noted by reviewer #1. We absolutely agree with your comment. Thus, we have deleted this inappropriate description and corrected this opinion throughout the paper. Please see in mms (Lines 524−527).

14. Lines 365-369: Was it influenced by the uncertainties of retrieval methods?

Reply: We have stated the potential influence of the uncertainties in the retrieval methods in the revised draft. Please see in mms (Lines 535−545).

Lines 535−545 in mms:

"In addition, the percentage of hydrometeors within the Z_{DR} columns is investigated on the basis of the retrieved contents of ice (including graupel) or raindrops, as described in Section 2b. The results of hydrometeor identification are dominated by large size particles. Thus, we count the grids of ice (graupel) or raindrops via the results of the Z_{DP} method to investigate the percentage of hydrometeors within the Z_{DR} columns, avoiding neglecting the grid that possesses both ice (graupel) particles and liquid drops simultaneously. The obvious phenomenon is that the percentage of graupel within the Z_{DR} columns suddenly peaks before the first peak of lightning activity, but the second peak of lightning activity is not related to the presence of graupel within the Z_{DR} columns; the hydrometeor type within the Z_{DR} column at 18:30 CST is raindrops (Figure 9). Notably, the results neglect raindrops that smaller than 1 mm; although these small raindrops are a minor within the Z_{DR} column."

15. Lines 394-395, 454-455: If ZDR is assumed as a predictor for lightning then how do you explain variation of lightning before peak ZDR column height? Does it contradict physics?

Reply: As two reviewers caution, the related content is based on a case study, and some results are not robust. Moreover, as noted by reviewer #1, from a practical point of view, the timing of the maximum correlation is less important than a trend toward confidence for lightning, so in that sense, the Z_{DR} signal is more helpful. Thus, we have revised the related content (replacing sections 3.3 and 3.4 with statistical results) and corrected the results on the basis of fifteen isolated thudnerstorms in the draft.

The statistical relationships between the polarimetric radar variables and lightning activity are shown in Figure 12, **Section 3.4**. Please see in mms (Lines 624−639).

Lines 624−639 in mms:

"Figure 12a shows that the variation in the graupel or rain water content above the melting level within the cloud can predict the lightning activity (total flashes) after 6 minutes well, and the correlation coefficient is approximately 0.8. However, other parameters (e.g., Z_{DR} column volume, ice content above the melting level, and graupel volume) also exhibit good performance in forecasting lightning activity, and the correlation coefficient can reach approximately 0.7. The graupel volume is calculated based on the identification results of hydrometeors. Although the variation in the graupel or rain water content above the melting level within the cloud can also forecast the lightning activity (CG flashes) after 6 minutes, the correlation coefficient decreases to approximately 0.56 (Figure 12b). Notably, the trend of the Z_{DR} column volume implies that it may perform well with a longer warning time (e.g., 12 minutes) for lightning activity.

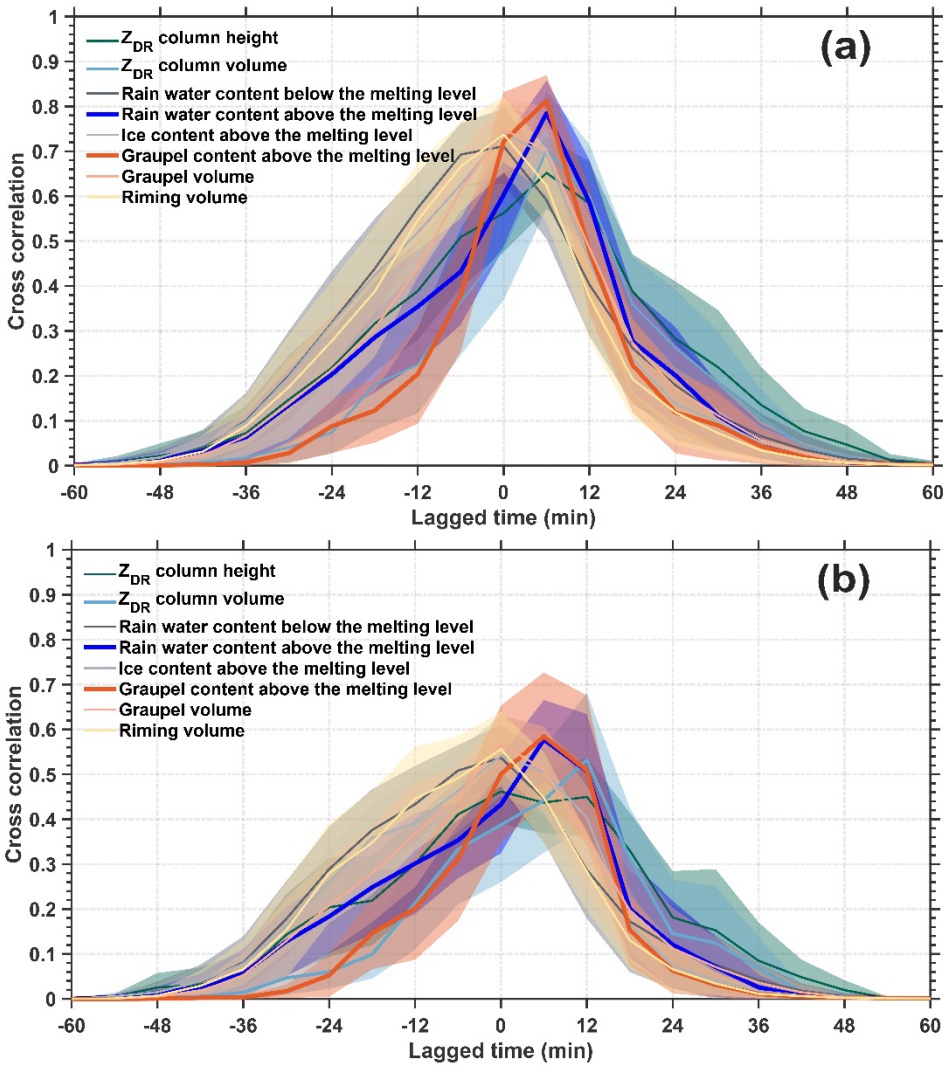

Figure 12. Cross-correlations between flash frequency (total flashes (a), CG flashes (b)) and eight radar-retrieved variables (Z_{DR} column height/volume, rain water content below/above the

melting level, ice content above the melting level, graupel content above the melting level, graupel volume, and riming volume); the lines indicate the mean values and the shaded area indicates the 95% confidence interval. The lagged time is for flash frequency lags these eight radar-retrieved variables."

16. Line 394, 406, 415, 422, 424, 425: Reporting 6 minutes as lightning prediction time is ambiguous due to lack of uncertainty quantifications. Simple methods such as implementing confidence intervals (may use bootstrapping) and hypothesis testing are needed for robust analysis of the cross-correlation.

Reply: We have revised the related content (replacing sections 3.3 and 3.4 with statistical results) and corrected the results on the basis of fifteen isolated thudnerstorms in the draft.

The statistical relationships between the polarimetric radar variables and lightning activity are shown in Figure 12, **Section 3.4**. Please see in mms (Lines 618−632). The 95% confidence intervals for the results are shown in Figure 12. The related content can be found in the last reply.

17. Lines 440-442: The manuscript lacked any discussion on the concept of "interactions." Could you please elaborate on how the authors managed to enhance our comprehension of the related cloud microphysics by solely examining the simple relationship between lightning flash frequency and ZDR or KDP column?

Reply: We have revised the draft; specifically, the detailed interactions of polarimetric structures and lightning activity related cloud microphysics and dynamics are investigated in **Section 3.2**. Please see in mms (Lines 451−508).

Lines 451−508 in mms:

"**3.2 Vertical structures of microphysics related to lightning activity**

To study the vertical thunderstorm structure related to lightning activity, we explore the vertical structures of polarimetric radar variables and microphysics, in combination with 3D lightning location data. Figure 7 displays the cross sections of polarimetric radar variables (Z_H, Z_{DR}, and K_{DP}) and microphysics (hydrometeor types and microphysical fingerprints) from the Cartesian grid of the studied isolated thunderstorm. At 18:00 CST (Figure 7 a1-e1), the lightning activity begins, and the locations of the flash sources are high and correspond mainly to graupel particles. Riming occurrence surrounds the flash sources. The Z_{DR} column and reflectivity core (≥ 40 dBZ) begin to separate, having previously been overlapping during the initial development stage of

the thunderstorm (Figure 4a, b). Then, at 18:06 CST (Figure 7 a2-e2), riming begins obviously, the echoes strengthen (≥ 55 dBZ), and the heights of the strong echoes are lifted. This finding indicates that the convective strength or updrafts are obviously increased and that the cold cloud processes are heavily. The lightning activity reached the first peak, where the locations of the flash sources mainly corresponded to graupel and ice particles. Moreover, the Z_{DR} column is located at the periphery of the reflectivity core, and high K_{DP} values occur and correspond to heavy rain particles, which are associated with large ice particles (e.g., hailstones) melting, raindrops coalescence and/or break. This phenomenon is consistent with that the K_{DP} tends to be directly proportional to the rain mixing ratio (Snyder et al., 2017).

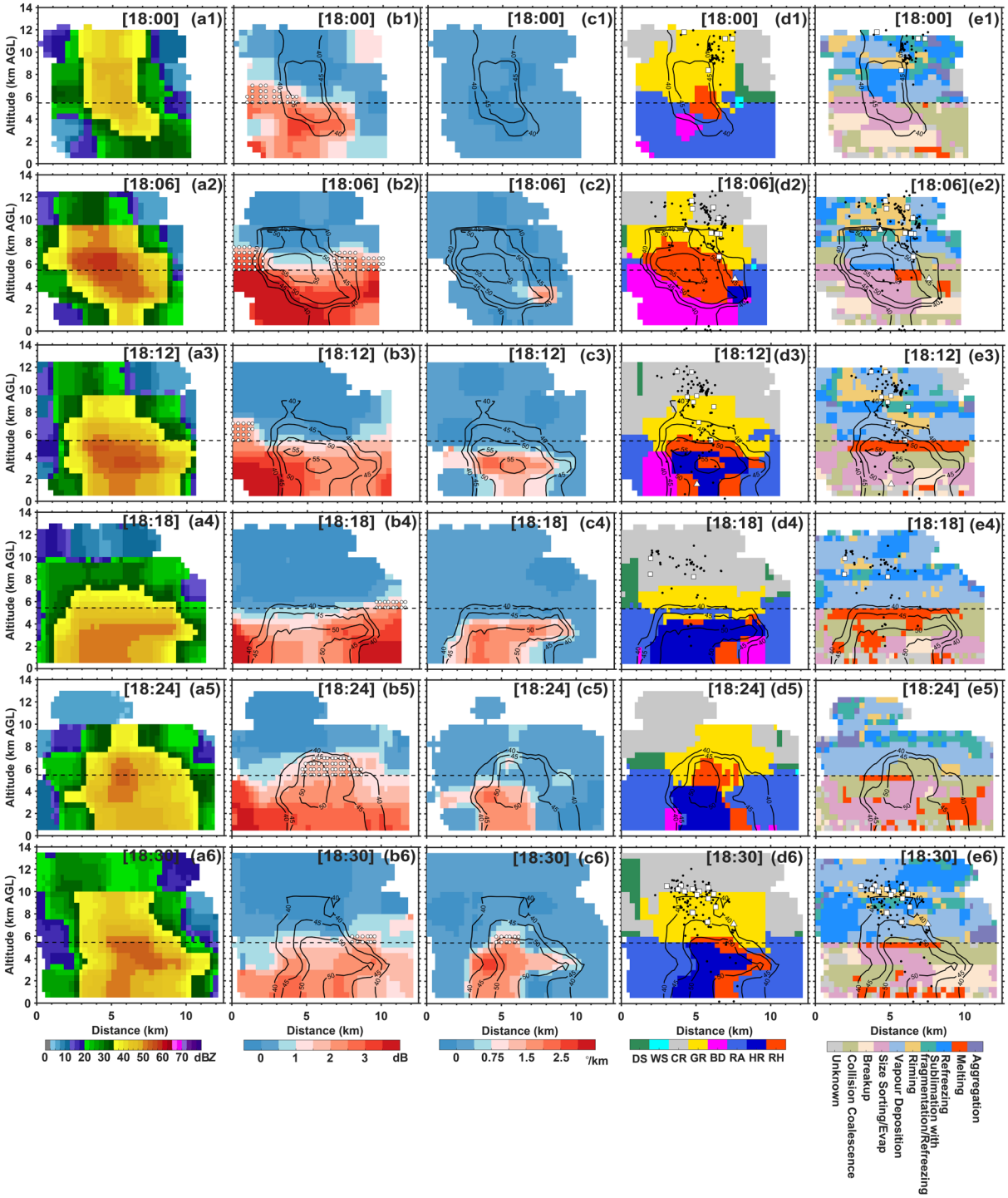

Figure 7. Cross sections of polarimetric radar variables (Z_H, Z_{DR}, and K_{DP}) and microphysics (hydrometeor types and microphysical fingerprints) from the Cartesian grid of the isolated thunderstorm (case #1). At 18:00 CST (a1-e1), 18:06 CST (a2-e2), 18:12 CST (a3-e3), 18:18 CST (a4-e4), 18:24 CST (a5-e5), and 18:30 CST (a6-e6). The black dashed line indicates the 0°C isotherm height. The white dots indicate the areas of the identified Z_{DR}/K_{DP} columns. The black contours with values indicate the reflectivity structure. The black dots indicate the flash

sources, the white square represents the first source of the intracloud flash, and the triangle represents the CG flash.

Subsequently, the lightning activity weakened at 18:12 and 18:18 CST. During this stage (Figure 7 a3-e3, a4-e4), the reflectivity core is landing and large ice particles above the melting level decrease, corresponding to heavy melting and indicating increasing downdrafts. Although Z_{DR} columns are present, they can only indicate updrafts around the reflectivity core. However, the reflectivity core was lifted again at 18:24 CST (Figure 7 a5). The contents of rain and hail mixtures and graupel clearly increased (Figure 7 d5). This indicates that the convective strength or updrafts are increased. Notably, the Z_{DR} column and reflectivity core overlap again, just as occurred during the initial development of the thunderstorm (Figure 4a, b; Figure 7 b5). Although a few high K_{DP} values occurred above the melting level, a K_{DP} column formed during the next 6 minutes (Figure 7 c5, c6). At 18:30 CST (Figure 7 a6-e6), the lightning activity reaches the second peak, and the riming process surrounds these flash sources. The Z_{DR} column within the reflectivity core quickly collapses with the occurrence of abundant graupel particles.

In total, this thunderstorm shows two impulses in vertical velocity, which correspond to two lightning activity peaks. When the first impulse event initially develops, the Z_{DR} column is obvious and overlaps with the reflectivity core; however, the region of the Z_{DR} column within the reflectivity core will collapse, with abundant graupel particles forming by riming or freezing, stimulating updrafts and intensified lightning. When large ice particles (e.g., graupel or hailstone) subsequently decrease, indicating the end of the first impulse event, melting and shedding processes occur, resulting in more raindrops (many moderate-to-large and small raindrops) contributing to high Z_{DR}/K_{DP} values. These raindrops could recirculate into the updrafts and be lifted to the mixed-phase region, forming the Z_{DR} column first, and raindrops could transfer to abundant graupel and even hailstones, releasing latent heat and thus invigorating updrafts again (indicating the second impulse event). However, the Z_{DR} column within the reflectivity core will collapse with increasing amounts of graupel and/or hailstone particles, but the K_{DP} column will occur; this can be explained by the increased K_{DP} values at the column top being associated with an increasing number of small-to-moderate hailstones with significant water fraction (Snyder et al., 2017). The lightning activity also reaches a peak value.

Thus, the Z_{DR} column within the reflectivity core is likely an indicator of imminent convection invigoration via latent heat release and then the formation of abundant graupel particles promotes lightning activity via noninductive charging; the K_{DR} column

is highly related to cold cloud processes, replacing Z_{DR} column to indicate updrafts within the reflectivity core when obvious graupels and hailstones occur."

18. Lines 469-472: The authors should examine whether the uncertainties of the retrieval methods and radar data spatial and temporal resolutions influence these results.

Reply: Yes. Thank you for your constructive suggestions. The limitations and uncertainties of the methods and data are discussed. We have added the related statement in **Sections 2 and 4**. The statistical results have been added to strengthen the conclusion. A statement about the uncertainties of the radar data can be found in mms (Lines 783−785). Other discussions can be found in the above replies and Lines 786−808).

Lines 783−785 in mms:

"In addition, the 6-min or 12-min warning time in our results is likely due to the temporal resolution (6 minutes) of the radar data used in this study; high temporal resolution observations of phased-array radar may decrease the uncertainty."

Lines 786−808 in mms:

"Notably, the threshold value for identifying the Z_{DR} column (≥1.5 dB) in this study is different from that (≥1 dB) in previous studies (e.g., Sharma et al., 2024). Although this threshold value is selected according to the retrieved raindrop diameter, which should exceed 2 mm within the Z_{DR} column during the initial phase of a storm (Kumjian, et al., 2014), the results for quantifying the Z_{DR} column (i.e., height and volume) may be different from those of previous studies that used the 1 dB threshold (e.g., Sharma et al., 2024). However, this study focuses on the trend of the Z_{DR} column height or volume; thus, the differences resulting from different thresholds are relieved. The threshold value for identifying the K_{DP} column (≥1°/km) in this study is consistent with that used by Sharma et al. (2024). However, the different estimation methods for K_{DP} may introduce additional uncertainty, as discussed in Sharma et al. (2021).

Moreover, the height of the melting layer (0°C), which is derived from environmental soundings, is assumed to be constant for identifying and quantifying the Z_{DR}/ K_{DP} column; however, the melting level is frequently elevated within updraft cores because of latent heat release, which is influenced by the strength of updrafts relative to the ambient environment. Thus, a more accurate melting level will decrease the biased estimations of the "3D mapping columns" method in this study. In addition, although our results support some observations in Bruning et al. (2024) and seem to

explain the remaining question in Sharma et al. (2024) and Sharma et al. (2021), whether there are differences between such small, isolated, subtropical thunderstorms and other thunderstorm types (i.e., mesoscale convective systems, supercells, or tropical thunderstorms) should be further analysed to reduce the probability of uncertainty in our study. Finally, although the results retrieved from hydrometeor identification and microphysical fingerprint methods are reasonable and obey theoretical cognition in this study, the potentially biased estimates may result from isothermal height and the status of the hydrometeor (e.g., canting angle)."

19. Lines 480-481: List the four parameters.

Reply: The sentence has been revised in the draft as suggested. Please see in mms (Lines 762−764).

Lines 762−764 in mms:

"We bridged the polarimetric structure (the Z_{DR}/K_{DP} column, supercooled liquid water, and graupel content below 0°C) and lightning activity on the basis of observations of fifteen isolated thunderstorm cells (the variation curve is conceptualized in Figure 13)."

20. Lines 480-483: Another objective of this study was to clarify the sequence and interactions of the four parameters mentioned for predicting lightning activity during the cloud life cycle (lines 440-442). Consequently, after their analysis, the authors propose the conceptual model presented in Figure 12, which is a key highlight of this article. However, a clear explanation of the processes underlying Figure 12 is lacking and should be included in the manuscript.

Reply: The sentence has been revised in the draft as suggested. Please see in mms (Lines 762−785).

Lines 762−785 in mms:

"We bridged the polarimetric structure (the Z_{DR}/K_{DP} column, supercooled liquid water, and graupel content below 0°C) and lightning activity on the basis of observations of fifteen isolated thunderstorm cells (the variation curve is conceptualized in Figure 13). The two peaks of lightning activity in Figure 13 suggest multiple impulse events in convection; specifically, the first peak refers specifically to the initial impulse event, but the second peak suggests subsequent impulse events. The magnitude of the amplitudes among these curves has no practical meaning; it is merely for visualization purposes.

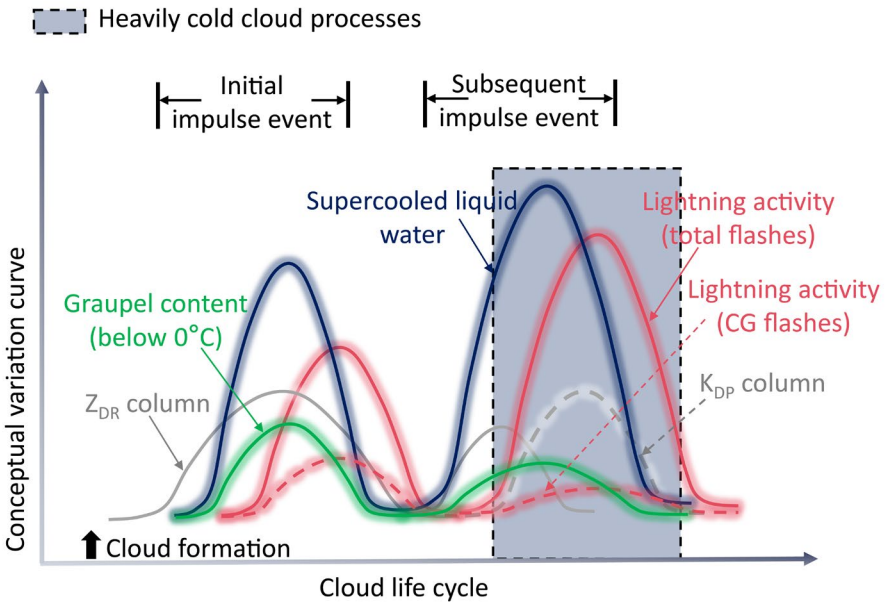

Figure 13. A conceptual model bridging the polarimetric structure and lightning activity.

In our opinion (Figure 13), the Z_{DR} column within the reflectivity core is likely an indicator of imminent convection invigoration via latent heat release, after which the formation of abundant graupel particles promotes lightning activity via noninductive charging. Therefore, microphysics (e.g., graupel content) are more directly related to lightning activity than are dynamics (e.g., the Z_{DR} column). Moreover, the observations reveal that the microphysical variations in supercooled liquid water and graupel yield better correlation coefficients for the prediction of lightning activity at short warning times (e.g., 6 minutes in this study) than do the dynamical variations in the Z_{DR} column volume. However, the trend of the Z_{DR} column volume implies that it may perform well with a longer warning time (e.g., 12 minutes in this study) for lightning activity. The K_{DR} column is highly related to cold cloud processes. Thus, the K_{DP} column is likely absent when the impulse event initially develops; however, it will be present later with heavily cold cloud processes, replacing the Z_{DR} column to indicate updrafts within the reflectivity core when obvious graupels and hailstones are occurring. In addition, the 6-min or 12-min warning time in our results is likely due to the temporal resolution (6 minutes) of the radar data used in this study; high temporal resolution observations of phased-array radar may decrease the uncertainty."

21. Lines 486-487: "the former" or the latter? Indicate it explicitly.

Reply: This confusing description has been deleted. Please see in mms (Lines 820−821).

22. Lines 492-493: Between lines 150 and 152 the authors explicitly state their intention to utilize this study for forecasting lightning activity within isolated thunderstorm cells over South China. However, they do not explicitly outline many uncertainties inherent in their study. For instance, one notable uncertainty involves determining the ZDR column height or volume based on an assumed freezing level derived from environmental soundings. The freezing level is frequently elevated within updraft cores due to latent heat release, which is influenced by the strength of updrafts relative to the ambient environment. This phenomenon can lead to biased estimations.

Reply: Thank you for your suggestion, which has improved this manuscript substantially. We have added a statement about the uncertainties of this "3D mapping columns" method. Please see in mms (Lines 786−808).

Lines 786−808 in mms:

"Notably, the threshold value for identifying the Z_{DR} column (≥1.5 dB) in this study is different from that (≥1 dB) in previous studies (e.g., Sharma et al., 2024). Although this threshold value is selected according to the retrieved raindrop diameter, which should exceed 2 mm within the Z_{DR} column during the initial phase of a storm (Kumjian, et al., 2014), the results for quantifying the Z_{DR} column (i.e., height and volume) may be different from those of previous studies that used the 1 dB threshold (e.g., Sharma et al., 2024). However, this study focuses on the trend of the Z_{DR} column height or volume; thus, the differences resulting from different thresholds are relieved. The threshold value for identifying the K_{DP} column (≥1°/km) in this study is consistent with that used by Sharma et al. (2024). However, the different estimation methods for K_{DP} may introduce additional uncertainty, as discussed in Sharma et al. (2021).

Moreover, the height of the melting layer (0°C), which is derived from environmental soundings, is assumed to be constant for identifying and quantifying the Z_{DR}/ K_{DP} column; however, the melting level is frequently elevated within updraft cores because of latent heat release, which is influenced by the strength of updrafts relative to the ambient environment. Thus, a more accurate melting level will decrease the biased estimations of the "3D mapping columns" method in this study. In addition, although our results support some observations in Bruning et al. (2024) and seem to explain the remaining question in Sharma et al. (2024) and Sharma et al. (2021), whether there are differences between such small, isolated, subtropical thunderstorms and other thunderstorm types (i.e., mesoscale convective systems, supercells, or tropical thunderstorms) should be further analysed to reduce the probability of uncertainty in our study. Finally, although the results retrieved from hydrometeor identification and microphysical fingerprint methods are reasonable and obey

theoretical cognition in this study, the potentially biased estimates may result from isothermal height and the status of the hydrometeor (e.g., canting angle)."

23. Figure 4: Considering the goal is to understand and predict lightning activity using ZDR column, why does Figure 4 not show and discuss observed characteristics of the ZDR column at 18:00 hours when the first lightning was detected?

Reply: We have added the related analysis in **Section 3.2**, including the observed characteristics of the Z_{DR} column at 18:00 CST. Please see in mms (Lines 456−460).

Lines 456−460 in mms:

"At 18:00 CST (Figure 7 a1-e1), the lightning activity begins, and the locations of the flash sources are high and correspond mainly to graupel particles. Riming occurrence surrounds the flash sources. The Z_{DR} column and reflectivity core (≥ 40 dBZ) begin to separate, having previously been overlapping during the initial development stage of the thunderstorm (Figure 4a, b)."

24. Figure 6: Explain the representation of colorbar. Fig. 6c should be D0 and Fig. 6d should be LWC.

Reply: Corrected. Please see in mms (Lines 528−534).

Lines 528−534 in mms:

"

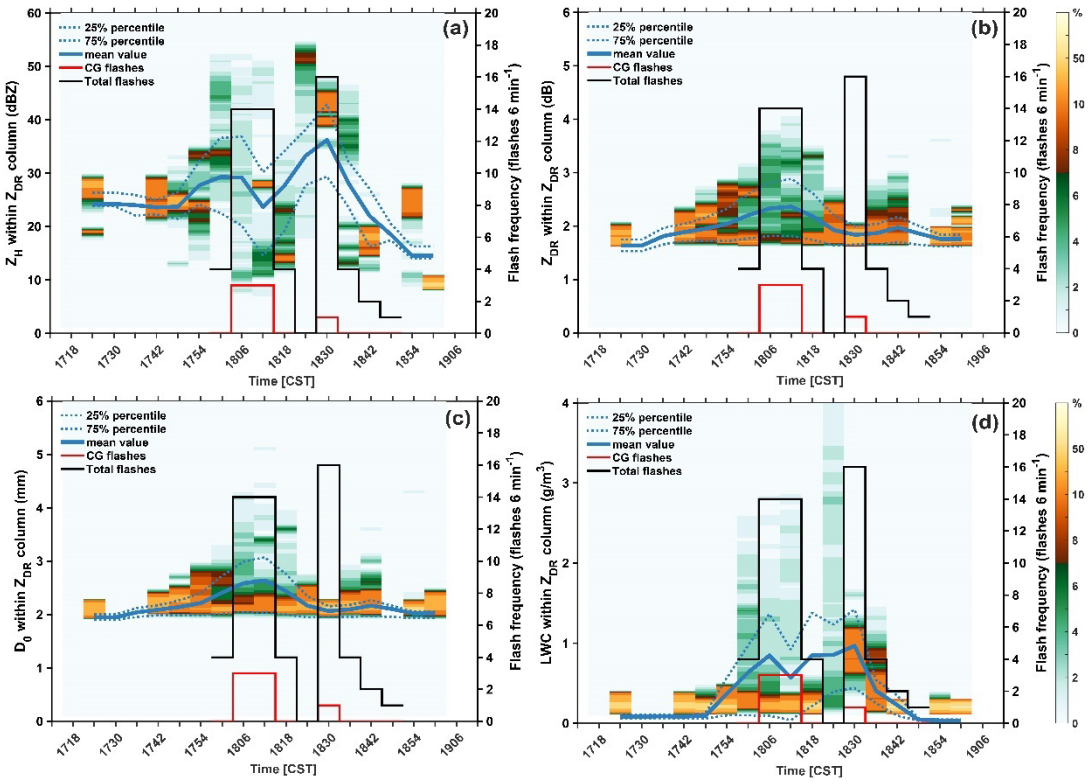

Figure 8. The normalized distributions of the polarimetric and microphysical characteristics within the series of Z_{DR} columns. (a) Z_H. (b) Z_{DR}. (c) Median volume diameter (D_0) of raindrops. (d) Liquid water content (LWC). The blue solid line indicates the mean value. The shading indicates the normalized occurrence frequency (unit: %). The blue dashed lines indicate the 25% and 75% percentiles. The black (red) stepped line indicates the total flashes (CG flashes) from LFEDA, and the lightning flash frequency is counted every 6 minutes."

25. Figure 8b: Is the lagged time for flash frequency or ZDR column height? It should be clarified in the figure caption.

Reply: This has been clarified in Figure 12. Please see in mms (Lines 634−639).

Lines 634−639 in mms:

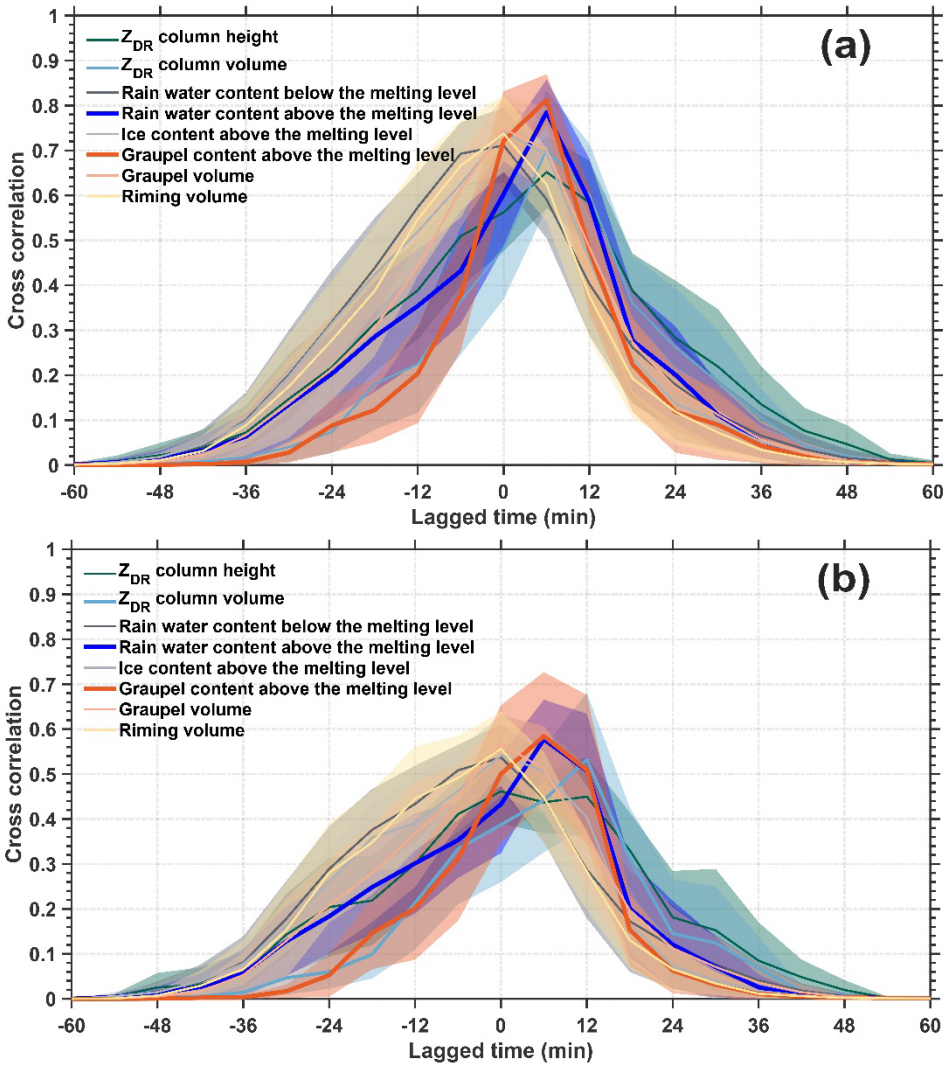

"

Figure 12. Cross-correlations between flash frequency (total flashes (a), CG flashes (b)) and eight radar-retrieved variables (Z_{DR} column height/volume, rain water content below/above the melting level, ice content above the melting level, graupel content above the melting level, graupel volume, and riming volume); the lines indicate the mean values and the shaded area indicates the 95% confidence interval. The lagged time is for flash frequency lags these eight radar-retrieved variables."

26. Figures 8b, 9b: Use different colors for total and CG flashes (avoid blue/orange) as it gets confusing later with figures 10 b, c and 11b, c when you use the same colors for below and above freezing levels. Using different line styles would also benefit to differentiate total and CG flashes.

Reply: These figures (Figures 8, 9, 10, and 11) have been replaced with Figure 12, with the statistical results. Please see in mms (Lines 634−639).

27. Figure 11: Choose different colors to show ice and graupel, as they both indicate retrievals above freezing level, using orange and blue is confusing here.

Reply: The same as in the last reply. These figures (Figures 8, 9, 10, and 11) have been replaced with Figure 12, with the statistical results. Please see in mms (Lines 634−639).

Technical Corrections:

1. Lines 44, 198: Define ZH, since using it for the first time in abstract and text respectively.

Reply: Corrected. Please see in mms (Line 241).

2. Line 79: "lighting" -> "lightning".

Reply: Corrected. Please see in mms (Line 89).

3. Lines 148-150: Mentioned four parameters at line 147, so either remove 3 bullets or add fourth bullet before word KDP columns.

Reply: This sentence has been rephrased. The term "dynamical and microphysical characteristics" has been used to replace "four parameters". Please see in mms (Lines 168−172).

4. Figure 5: Define "AGL" (Above Ground Level) in the caption. Also provide time zone details as [CST] on the x-axis label.

Reply: Corrected. The definition of "AGL" has been added to the corresponding figure captions, as have the time zone details.

5. Figures 6, 7, 8a, 9a, 10a, 11a: Provide time zone details on x-axis, Time [CST].

Reply: Corrected.

6. Lines 405-406: Do authors mean ZDR column volume? Could be a typo here.

Reply: Corrected.